GEOLOGICA CARPATHICA, 2026, 77, 4, 307–329 https://doi.org/10.31577/GeolCarp.2026.16

Geodynamic evolution of the Northernmost Dinarides revealed by the petrogenesis of Mid-Triassic calc-alkaline volcanic rocks

DAMIR SLOVENEC[1], DUJE KUKOČ[1,✉], DUJE SMIRČIĆ[2], BRANIMIR ŠEGVIĆ[3], MATIJA VUKOVSKI[1], MIRKO BELAK[1], TEA KOLAR-JURKOVŠEK[4], TONĆI GRGASOVIĆ[1], ŠPELA GORIČAN[5] and MARIJA HORVAT[1]

[1]Croatian Geological Survey, Sachsova 2, 10000 Zagreb, Croatia
[2]Faculty of Mining, Geology and Petroleum Engineering, University of Zagreb, Pierottijeva 6, 10000 Zagreb, Croatia
[3]Department of Geosciences, Texas Tech University, 1200 Memorial Circle, Lubbock 79409 TX, U.S.A.
[4]Geological Survey of Slovenia, Dimičeva ulica 14, 1000 Ljubljana, Slovenia
[5]Ivan Rakovec Institute of Paleontology, ZRC SAZU, Novi trg 2, 1000 Ljubljana, Slovenia

(Manuscript received February 3, 2026; accepted in revised form June 2, 2026; Associate Editor: Igor Broska)

Abstract: This paper presents mineralogical, petrological, geochemical, and Sr–Nd isotopic data on volcanic rocks from the Northwestern Croatian Triassic Rift Basin, which is a locally aborted back-arc rift system of the Paleotethys. The dataset also includes their isotopic ages, along with the biostratigraphic ages of all interbedded sedimentary rocks. These volcano-sedimentary successions represent the northernmost parts of the Dinarides. The obtained $^{40}Ar/^{39}Ar$ isotopic age (243±1.8 Ma) indicates the Late Anisian age of the basaltic eruption and is somewhat consistent with the obtained Early Ladinian biostratigraphic ages of the interbedded sedimentary rocks. The initial ε_{Nd} varies between −0.08 to +1.90, while the initial $^{87}Sr/^{86}Sr$ varies in a wide range from 0.704765 to 0.709248. The investigated Late Anisian to Early Ladinian calc-alkaline/shoshonitic basaltic lavas were formed through: (i) low-degree partial melting (5–14 %) of a shallow (spinel stability facies; max. depth ~33 km) magma source region in the subcontinental lithospheric mantle and (ii) fractional crystallisation in a partially open magmatic system. The magma generation also involved: (i) melts from the subducted slab, which is likely linked to the ancient, subducted oceanic crust of the Paleotethys, (ii) less abundant, previously subducted continental crustal material – sediments recycled in the mantle wedge, and (iii) a negligible contribution from depleted or an ocean-island, basalt-like mantle. These conditions suggest that the magma formed through a complex process during magma ascent through tectonically weakened crustal zones. Although the intense effusive volcanic activity during the Middle Triassic in the Northwestern Croatian Triassic Rift Basin lasted for a relatively short period (~3–4 Myr; Bithynian–Fassanian), its geodynamic evolution was complex and can be attributed to: (i) the subduction of the Paleotethyan lithosphere associated with an ensialic volcanic arc developed in an active continental margin setting, and (ii) the processes of continental rifting along the mid-Triassic margins of the Adria Plate, i.e., Greater Adria. These processes represent the beginning of rifting, which affected a greater area on the Balkan Peninsula as well.

Keywords: Middle Triassic, calc-alkaline volcanism, basalt suite, northernmost segment of the Dinarides, NW Croatia and E Slovenia

Introduction

The Mediterranean region, which represents the plate boundary zone between the African and Eurasian plates, is characterised by a complex geodynamic evolution (e.g., Stampfli & Borel 2002, 2004; Şengör 2009; van Hinsbergen et al. 2020; van Hinsbergen & Schouten 2021) and diverse magmatic activity that occurred in the Tethyan realm (Paleotethys, Neotethys) during the Triassic, particularly during the Middle Triassic (Pamić 1984; Castellarin et al. 1988; Serri et al. 2001; Goričan et al. 2005; Pamić & Balen 2005; Storck et al. 2018; Lustrino et al. 2019). Middle Triassic magmatism, which is predominantly represented by multi-phase lava flow extrusions and various types of pyroclastic rocks, as well as rare intrusions of intrusive rocks, is widely distributed across the Adria Plate, including the Alpine–Carpathian Belt, such as the Trans-Danubian region, Bükk Mountains, Southern Alps, Dinarides, and the Hellenides (Pamić 1984; Castellarin et al. 1988; Bonadiman et al. 1994; Harangi et al. 1996; Pe-Piper 1998; Pomonis et al. 2004; Beccaluva et al. 2005; Goričan et al. 2005; Velledits 2006; Graciansky et al. 2011; Haas et al. 2011; Saccani et al. 2015; Bianchini et al. 2018; Casetta et al. 2018, 2019; Smirčić et al. 2018; Storck et al. 2018; Lustrino et al. 2019; Castorina et al. 2020; De Min et al. 2020; Slovenec et al. 2020, 2023a, b; Slovenec & Šegvić 2021; Velicogna et al. 2023; Ogunyele et al. 2024; Nardini et al. 2025; Visona et al. 2025). However, the geodynamic model and tectonomagmatic evolution of these areas in the former western segment

✉ corresponding author: Duje Kukoč
dkukoc@hgi-cgs.hr

of the Paleotethys, which once separated Gondwana and Laurussia, as well as the petrogenesis of the magmatic rocks exposed there, still remain subjects of debate (Şengör 1984, 2009; Stampfli & Borel 2004; Bortolotti & Principi 2005; Bortolotti et al. 2013; Stampfli et al. 2013; Zulauf et al. 2018; Neubauer et al. 2019; De Min et al. 2020; van Hinsbergen et al. 2020; Ogunyele et al. 2024; Slovenec & Šegvić 2024; Spahić 2024). Thus, the origin of Middle Triassic magmatism in the Mediterranean region is often associated with continental rifting-related processes (Crisci et al. 1984; Pamić 1984; Pamić & Balen 2005; Dal Piaz & Martin 1998; Aljinović et al. 2010; Saccani et al. 2015; Lustrino et al. 2019; De Min et al. 2020; Slovenec et al. 2020, 2023a, b; Ogunyele et al. 2024; Visonà et al. 2025) or alternatively, with convergent tectonics associated with the subduction of the Paleotethys (Bébien et al. 1978; Castellarin et al. 1980, 1988; Obenholzner 1991; Bonadiman et al. 1994; Stampfli & Borel 2002, 2004; Schmid et al. 2004; Trubelja et al. 2004; Grimes et al. 2015; Bianchini et al. 2018; Casetta et al. 2018; Smirčić et al. 2018; Storck et al. 2018; Castorina et al. 2020; Slovenec & Šegvić 2021).

Deposits of the incipient continental margin of the Adria Plate are preserved as segments of Middle Triassic volcano-sedimentary successions and can be found in the intra-Pannonian mountains of northwestern Croatia and eastern Slovenia (Figs. 1a and 2). These volcano-sedimentary successions now represent the northernmost part of the Dinarides (Vukovski et al. 2024), which crop out in the western segment of the Zagorje–Mid-Transdanubian Zone (ZMTDZ; *sensu* Pamić & Tomljenović 1998; Fig. 1b). The volcano-sedimentary successions of this zone, which belong to the Northwestern Croatian Triassic Rift Basin (NCTRB; Kukoč et al. 2023), are made of basic to felsic volcanic and pyroclastic rocks, as well as volcaniclastic deposits intercalated with deep-sea siliceous and carbonate sediments (e.g., Golub & Brajdić 1968, 1970; Golub et al. 1969; Šebečić 1969; Marci et al. 1982, 1984; Šimunić et al. 1982; Šimunić & Šimunić 1997; Goričan et al. 2005; Slovenec et al. 2020, 2023a, b; Slovenec & Šegvić 2021; Balen et al. 2022; Kukoč et al. 2023; Smirčić et al. 2024). Systematic investigation of the Middle Triassic volcano-pyroclastic sequence, which is spatially associated with sedimentary rocks of the NCTRB, is therefore of key importance for the reconstruction of magmatic activity, as well as for the interpretation of the multiphase lithospheric geodynamic processes that occurred along the continental margins of the Adria Plate, i.e., the northwestern segment of the Paleotethys.

In this study, we investigated Middle Triassic volcanism and the associated sedimentary rocks in the area of northwestern Croatia and eastern Slovenia. The research results present new mineralogical, petrological, geochemical, isotopic, and geochronological data of representative samples of effusive rocks, as well as biostratigraphic and sedimentological data from interstratified sediments, to formulate an integrated interpretation of calc-alkaline volcanism in this region and propose an original tectonomagmatic model for geodynamic evolution during the Middle Triassic.

Geological setting

The research area represents the northernmost segment of the Dinarides, which is a mountain range that runs along the eastern coast of the Adriatic Sea (Fig. 1). The Dinarides comprise several SW-verging tectono-stratigraphic units formed in response to convergence between the Adria Plate or Greater Adria (*sensu* van Hinsbergen et al. 2020) and the Eurasian plate (Schmid et al. 2008, 2020). Here, however, the Dinaridic structures bend sharply from their NW–SE trend and are laterally extruded towards the northeast along the Zagorje–Mid-Transdanubian Zone (ZMTDZ; *sensu* Pamić & Tomljenović 1998) or the Mid-Hungarian Fault Zone (*sensu* Csontos & Nagymarosy 1998; Ustaszewski et al. 2009) (Fig. 1b). Vukovski et al. (2024) attributed the successions investigated in this work to the Pre-Karst and Bosnian Flysch Unit (*sensu* Schmid et al. 2008), which is a first-order tectono-stratigraphic unit of the Dinarides comprising Triassic carbonates (mostly shallow-marine) and a Jurassic–Cretaceous platform margin and basin successions.

In the research area, which is largely covered by Cenozoic deposits of the Pannonian Basin, Mesozoic formations are exposed within a mountain chain representing an approximately 100 km long Rudnica–Ivanščica anticline (*sensu* Placer 1999), extending from eastern Slovenia into northern Croatia (Fig. 2a, b). These mountains are built of Triassic dolostones (Šimunić et al. 1981, 1982; Aničić & Jureša 1984, 1985) with local occurrences of basaltic to rhyolitic volcanic and pyroclastic lithologies, sometimes intercalated with radiolarian cherts and pelagic limestones of Middle Triassic age (Fig. 2a, b; e.g., Goričan et al. 2005; Slovenec et al. 2020, 2023a, b; Slovenec & Šegvić 2021; Kukoč et al. 2023; Smirčić et al. 2024). A younger Mesozoic sedimentary succession is exposed only on Ivanščica Mt. and includes thick Jurassic to Lower Cretaceous shallow- to deep-marine deposits found in tectonic contact with the ophiolitic mélange (Fig. 2a; Vukovski et al. 2023).

Paleogeographically, these stratigraphic successions are interpreted as originating from the Adria Plate or Greater Adria, which during the Middle Triassic was affected by intense rifting linked to the opening of the northern branch of the Neotethys Ocean (Kukoč et al. 2023; Slovenec et al. 2023a). Extension during this period created short-lived grabens, which were filled with pelagic sediments, volcanic and pyroclastic deposits, and separated by active carbonate platforms (Goričan et al. 2005; Slovenec et al. 2020, 2023b; Kukoč et al. 2023). These volcanic and pyroclastic lithologies are products of bimodal volcanic activity that generated submarine basaltic extrusions and explosive rhyolitic eruptions (Slovenec et al. 2023a; Smirčić et al. 2024). Following the rifting phase, this part of the Adriatic microplate represented a passive continental margin facing the evolving Neotethys to the north-east and was involved in the subsequent orogenic processes related to the closure of the Neotethys (Vukovski et al. 2023, 2024).

Structural relations in the research area are predominantly the result of nappe stacking during the Early Cretaceous,

Fig. 1. (a) Topographic map of Alps, Dinarides, and Pannonian Basin. **(b)** Simplified tectonic map of Schmid et al. (2020) showing major tectonic units of the Dinarides, Alps, Carpathians, and Tisza. **(c)** Detail from the figure 1b, modified according to Vukovski et al. (2024, 2026). The investigated areas (marked with two black rectangles) occupy a position at the northernmost part of the Dinarides close to the tectonic units of the Alps to the north, in the southwestern part of the Pannonian Basin (white outlines). ZMTDZ=Zagorje–Mid-Transdanubian Zone; PFS=Periadriatic Fault System; MHFZ=Mid-Hungarian Fault Zone.

which was caused by the closing of the Neotethys, with nappes composed of Adriatic margin successions and obducted Neotethyan ophiolites (Vukovski et al. 2024). Tectonic escape and its associated clockwise rotation in the Cenozoic related to the evolution of the Pannonian Basin brought these units from their original position, which was parallel to the structural trend of the Dinarides, into their present-day position (Tomljenović et al. 2008; Márton et al. 2002).

Middle Triassic volcano-sedimentary successions of NW Croatia

The Middle Triassic volcanic and pyroclastic lithologies of northwestern Croatia are intercalated within pelagic sedimentary successions ranging from the outer margin and upper slope to open-marine deposits (Fig. 3; Goričan et al. 2005; Slovenec et al. 2020, 2023a; Kukoč et al. 2023). Contact with the underlying and overlying, predominantly dolomitic lithologies is largely covered; however, a gradual transition from shallow-marine carbonate platform to basin is also recorded (Goričan et al. 2005). Thin-bedded micritic or recrystallised limestone, as well as red radiolarian chert are the dominant sedimentary lithologies in these successions. Limestone is often laminated and contains thin-shelled bivalves (filaments), calcified radiolarians and sponge spicules, and occasionally ammonites (Goričan et al. 2005; Kukoč et al. 2023). Coarse- and fine-grained resedimented carbonate lithologies are present locally. These lithologies contain shallow-marine carbonate

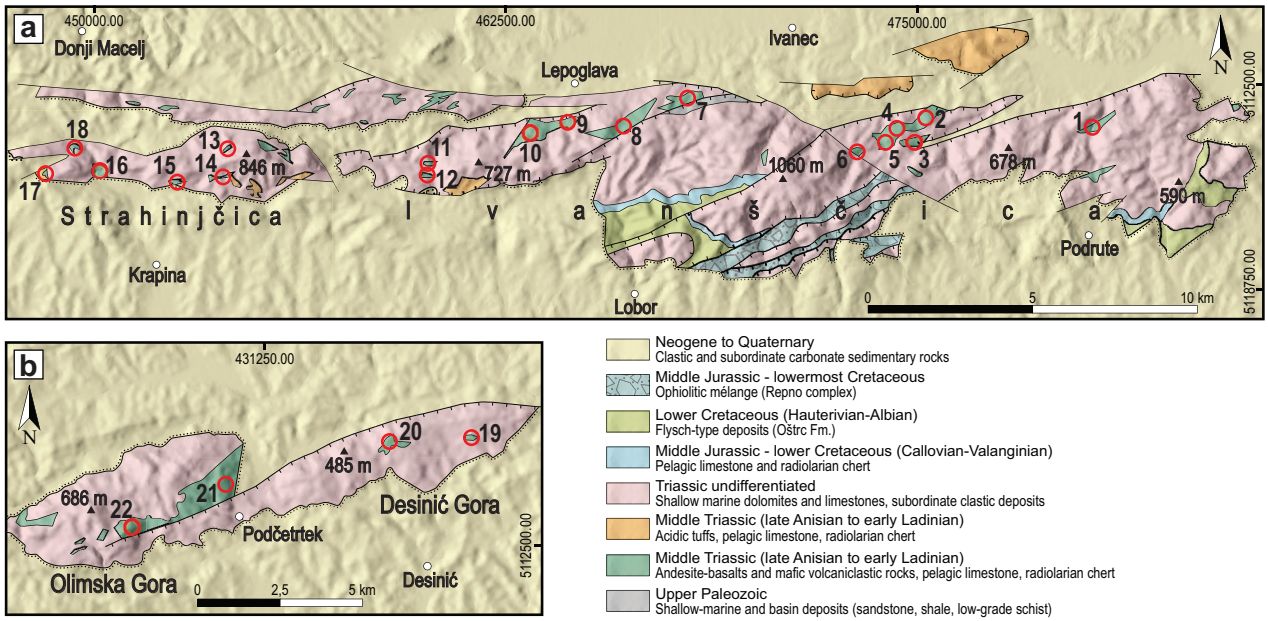

Fig. 2. Simplified geological maps of the Mts. **(a)** Ivanščica, Strahinjščica and Desinić Gora and **(b)** Mt. Olimska Gora (simplified according to Šimunić et al. 1982 and Aničić & Jureša 1984). The numbers indicate the locations of the analysed samples shown in Supplementary Tables S1–S4.

material, including algae, benthic foraminifers and reef-building fossils, as well as clasts of basalt and andesite–basalt in a pelagic carbonate matrix (Goričan et al. 2005; Kukoč et al. 2023). An Illyrian-Fassanian age of these deposits has been determined based on extracted conodont and radiolarian assemblages (Goričan et al. 2005; Slovenec et al. 2020; Kukoč et al. 2023). Ammonites found in one locality indicate that pelagic sedimentation began as early as the Pelsonian (Kukoč et al. 2023).

Materials and analytical techniques

The research area includes 22 locations on the Ivanščica, Strahinjščica, and Desinić Gora Mts. in Croatia, as well as Olimska Gora Mt. in Slovenia (Fig. 2a, b). In addition to point-sampled volcanic and sedimentary (carbonate and siliciclastic) rock samples, four geological columns were reconstructed (Fig. 3), which were thoroughly analysed from lithostratigraphic and biostratigraphic perspectives, including facies interpretation and determination of microfossil content (conodonts). Out of 237 collected volcanic rock samples from surface outcrops, 185 samples were selected for petrographic investigation. After microscopic selection, 34 representative samples were chosen for further analytical procedures.

The mineral compositions of four representative lava samples (Supplementary Table S1) were analysed at the University of Geneva's Department of Earth Sciences using a JEOL JXA 8200 Superprobe equipped with five wavelength dispersive spectrometers. Operating parameters included an accelerating voltage of 20 kV, a 15 nA beam current, and a defocused beam of ~10 µm. Counting times of 30 s on the peak and 15 s in the background on both sides of the peak were used for all elements, except for Na and K, which were measured for 20 s and 10 s on the peak and background, respectively, due to their high mobility under an electron beam. For this reason, Na and K were also measured first. Limits of detection (LOD) were calculated as the minimum concentration required to produce count rates three times higher than the square root of the background (3σ; 99 wt.% degree of confidence at the lowest detection limit). Concentrations below the LOD are reported as undetected. Raw data were corrected for matrix effects using the φρZ method by Armstrong (1991). Natural minerals, oxides (corundum, spinel, hematite and rutile) and silicates (albite, orthoclase, anorthite and wollastonite) were used as standard for calibration. Mineral formulas were calculated using the software package MINPET written by Linda R. Richard (Gatineau, Québec, Canada). Thirty-one representative lava samples were selected for the bulk-rock chemical analysis (Supplementary Table S2). Bulk-rock powders were obtained from rock chips free of veins/amygdales and analysed by XRF for major elements, and ICP-MS for trace elements at Texas Tech University's Department of Geosciences. Accuracy and precision were assessed using the USGS BHVO-2 analytical glass standards (Jochum 2005; for details see Šegvić et al. 2023b). Major and trace elements concentrations were measured with accuracy and precision better than ±1 % and ±5 %, respectively. It is 3σ at 10 times detection limit. Detection limits were as follows: TiO_2, MnO=0.001 wt.%; SiO_2, Al_2O_3, Fe_2O_3, MgO, CaO, Na_2O, K_2O, P_2O_5=0.01 wt.%; Lu=0.002 ppm; Eu=0.005 ppm; Ta, Pr, Sm, Gd, Ho, Er, Yb, U=0.01 ppm; Th, La, Ce, Nd, Tm=0.05 ppm; Cs,

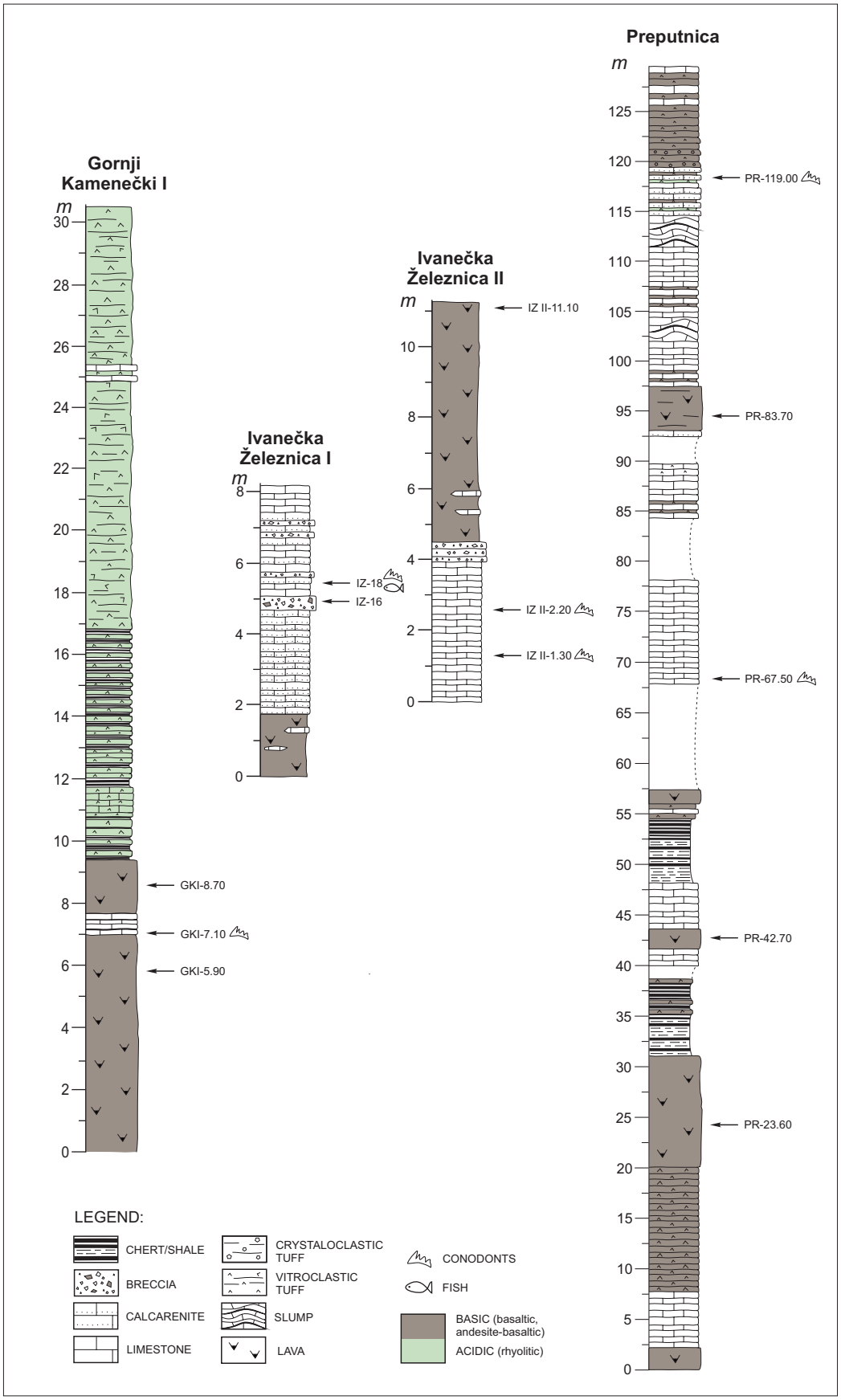

Fig. 3. The position of analysed samples on lithological columns of the investigated area. Lithological columns' location (see Fig. 2a): 2=Ivanečka Železnica I; 3=Ivanečka Železnica II; 6=Preputnica and 14=Gornji Kamenečki I.

Hf=0.1 ppm; Nb=0.2 ppm; Y=0.5 ppm; Sc, Rb, Zr=1 ppm; Sr=2 ppm; Ba=3 ppm; V, Pb=5 ppm; Cr, Ni=20 ppm. The quality of the measurements was checked by replicating the analysis on ~12 % of the samples.

Neodymium and strontium isotope compositions of twelve bulk rock lava samples (Supplementary Table S3) were measured at the Noble Gas Laboratory Pacific Centre for Isotopic and Geochemical Research, University of British Columbia using a Triton Plus mass spectrometer. Normalising ratios of $^{146}Nd/^{144}Nd=0.7219$ and $^{86}Sr/^{88}Sr=0.1194$ were assumed. The average JNd-i standard run at $^{143}Nd/^{144}Nd=0.512079 \pm 0.000008$ (n=22, 2σ). The data is reported relative to the recommended value of $^{143}Nd/^{144}Nd=0.512115$ (Tanaka et al. 2000). The BCR-2 USGS standard run at $^{143}Nd/^{144}Nd=0.512642 \pm 0.000008$, within error identical to the reference value of $^{143}Nd/^{144}Nd=0.512637 \pm 0.000012$ (Weis et al. 2006). The $^{87}Sr/^{86}Sr$ ratio for the NBS 987 Sr standard for the period of measurement was 0.710242 ± 0.000030 (n=92, 2σ). Total procedural blanks were ~500 pg and ~150 pg for Sr and Nd, respectively.

Plagioclase separates from andesite–basalt sample TSI-11 for $^{40}Ar/^{39}Ar$ analysis was separated by electromagnetic separator and standard heavy liquid techniques, and the less altered crystals were hand picking under a stereomicroscope. The plagioclase separates were wrapped in Al foil and stacked in an irradiation capsule with similar-aged samples and neutron flux monitors (Fish Canyon Tuff sanidine), 28.201±0.046 Myr (Kuiper et al. 2008). Samples were irradiated at the McMaster Nuclear Reactor and analysed at the Noble Gas Laboratory Pacific Centre for Isotopic and Geochemical Research, University of British Columbia. The mineral separates were step-heated at incrementally higher powers in the defocused beam of a 10W CO_2 laser (New Wave Research MIR10) until fused. The gas exolved from each step was analysed by a VG5400 mass spectrometer equipped with an ion-counting electron multiplier. All measurements are corrected for total system blank, mass spectrometer sensitivity, mass discrimination, radioactive decay during and subsequent to irradiation, as well as interfering Ar from atmospheric contamination and the irradiation of Ca, Cl and K (Isotope production ratios: $(^{40}Ar/^{39}Ar)_K = 0.0302 \pm 0.00006$, $(^{37}Ar/^{39}Ar)_{Ca} = 1416.4 \pm 0.5$, $(^{36}Ar/^{39}Ar)_{Ca} = 0.3952 \pm 0.0004$, $Ca/K = 1.83 \pm 0.01 (^{37}Ar_{Ca}/^{39}Ar_K)$). Initial data entry and calculations were carried out using the software ArArCalc (Koppers 2002). The plateau and isochron ages were calculated using ISOPLOT ver. 3.09 (Ludwig 2003). Errors are quoted at the 2σ (95 % confidence) level and are propagated from all sources except mass spectrometer sensitivity and age of the flux monitor. The data are shown in Supplementary Table S4.

Conodont analyses were carried out on 5 carbonate samples (Supplementary Table S5) with an average weight of 2 kg at the Geological Survey of Slovenia. Standard laboratory techniques with the use of diluted acetic acid (ca. 7–10 %) were utilised. Fossil collecting was performed manually under a stereoscopic microscope. All samples proved to be positive for conodonts, and one sample (IZ-18) also yielded fish remains.

Results

Sedimentary lithologies and biostratigraphy

Three new successions were studied, namely Ivanečka Železnica I and II and Preputnica (Fig. 3). The dominant sedimentary lithology in these successions is thin-bedded micritic limestone, often horizontally laminated and occasionally containing filaments. This limestone is recrystallised in places. Lithoclastic limestones (*sensu* Flügel 2010), which occasionally contain ooids, are present in all of the studied successions. Clast-supported, as well as matrix-supported breccias containing resedimented shallow-marine material and clasts of basalt are present (Fig. 3). When present, the matrix of these breccias is composed of lime mud and sometimes contains fine-ash sized vitroclastic particles. Fragments of micritic limestone are also occasionally observed within some of the investigated lavas, displaying thin, recrystalised rims only on rare occasions, thus indicating thermal contacts at the interface with the host magma. Chert and shale are present only in the Preputnica section. Mafic volcanic rocks are dominant (Figs. 3 and 4a–c), while beds of basic pyroclastic rocks represented by fine- to coarse-sized ash tuffs are found locally (Fig. 3).

The biostratigraphic dating of conodont faunas follow the data according to Chen et al. (2015) and Kolar-Jurkovšek & Jurkovšek (2019), although several more recent works were also taken into account. The colour of the conodont elements is black or grey and corresponds to a CAI (Colour Alteration Index) value of 5 or 6 (Epstein et al. 1977; Rejebija et al. 1987), which indicates a low degree of ocean floor metamorphism (Winkler 1979; Gawlick et al. 1994). The preservation of the found conodonts is moderate to poor; the specimens in sample IZ-18 are also altered (deformed) and indicate a metamorphic process (Harris et al. 1987). The recovered conodont assemblages are characterised by the elements belonging to five genera. The list of determined taxa includes: *Buduro-vignathus* sp., *Cratognathodus multihamatus* (Huckriede), *Gladigondolella tethydis* (Huckriede), *Gladigondolella* sp., *Neogondolella constricta* (Mosher and Clark), *Paragondolella alpina* (Kozur and Mostler), *P. eotrammeri* (Krystyn), *P.* aff. *eotrammeri*, *P. excelsa* Mosher, *P.* cf. *excelsa*, *P.* aff. *hanbulogi* Sudar and Budurov, *P. trammeri* (Kozur), *P. trammeri* and *Paragondolella* sp. (Fig. 5; Supplementary Table S5). *P. hanbulogi* was originally described from the uppermost Pelsonian (Sudar & Budurov 1979) and has been extensively reported from the Anisian sediments across the Dinarides (Kolar-Jurkovšek 1983; Sudar 1986; Sudar et al. 2013, 2023; Mrdak et al. 2024). The species *N. constricta, P. alpina, P. eotrammeri* and *P. trammeri* are well-known Anisian–Ladinian taxa, and all of them appear as early as the Illyrian (Chen et al. 2015). Additionally, the species *P. excelsa* is abundantly represented in the Middle Triassic fauna, but it has a slightly shorter stratigraphic range, i.e., from the upper Illyrian to the Fassanian. The most common species in the studied samples is *P. trammeri* (Kozur), which was recognised in two samples, however, it is questionable in the third sample.

In the conodont zonation of Slovenia, *P. trammeri* zone ranges from the upper Illyrian to the lower Fassanian (Kolar-Jurkovšek & Jurkovšek 2019). *Cratognathodus multihamatus* and *Gladigondolella tethydis* have limited stratigraphic importance due to a wider range. Both species range from the upper Spathian or lower Anisian to the Carnian (Koike 1999; Chen et al. 2015). According to Chen et al. (2015), the genus *Cratognathodus* is synonymous to *Gladigondolella*. *Budurovignathus* is a typical Ladinian taxon with rare representation in the lowermost Carnian (Rigo et al. 2018; Kolar-Jurkovšek & Jurkovšek 2019). The composition of the recovered conodont assemblages allowed us to determine the Illyrian (sample IZ-18), Upper Illyrian-Lower Fassanian (samples PR-67.50, IZ II-2.20), Ladinian (sample IZ II-1.30), and Middle Triassic ages of the samples. It should be noted here that *Gladigondolella, Paragondolella trammeri*, and *Budurovignathus* are all open-marine, pan-Tethyan taxa (Chen et al. 2015).

Petrography and mineral chemistry

The volcanic rocks of the investigated area are represented by massive lavas with irregular to plate-like jointing (Fig. 4a, b), occasionally by pillow lavas as well (Fig. 4c). The chemical composition of the mineral phases is shown in Supplementary Table S1. The studied lavas are dominated by a porphyritic to glomeroporphyritic texture and massive structure (Fig. 4d–h),

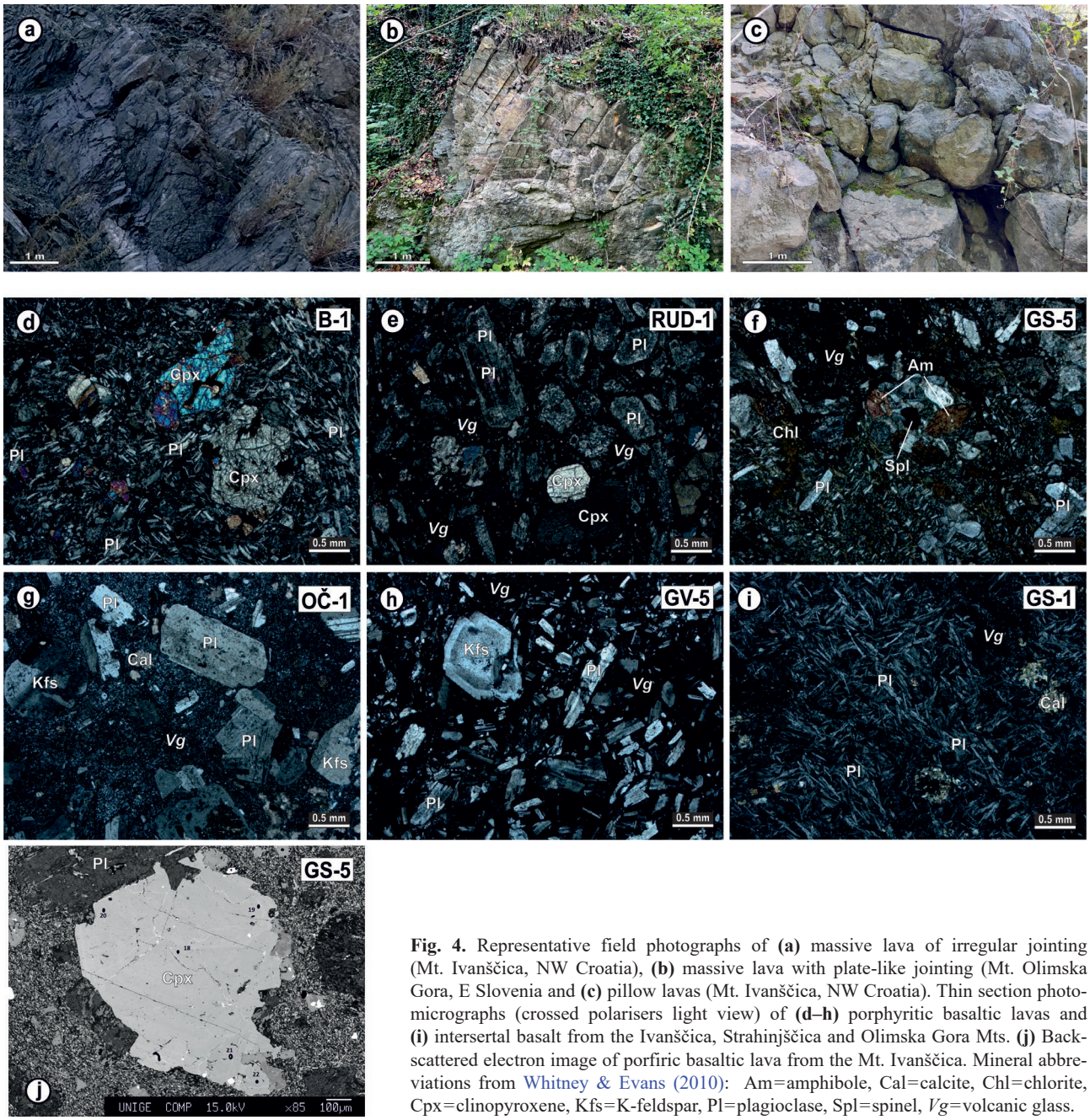

Fig. 4. Representative field photographs of **(a)** massive lava of irregular jointing (Mt. Ivanščica, NW Croatia), **(b)** massive lava with plate-like jointing (Mt. Olimska Gora, E Slovenia and **(c)** pillow lavas (Mt. Ivanščica, NW Croatia). Thin section photomicrographs (crossed polarisers light view) of **(d–h)** porphyritic basaltic lavas and **(i)** intersertal basalt from the Ivanščica, Strahinjščica and Olimska Gora Mts. **(j)** Back-scattered electron image of porfiric basaltic lava from the Mt. Ivanščica. Mineral abbreviations from Whitney & Evans (2010): Am=amphibole, Cal=calcite, Chl=chlorite, Cpx=clinopyroxene, Kfs=K-feldspar, Pl=plagioclase, Spl=spinel, *Vg*=volcanic glass.

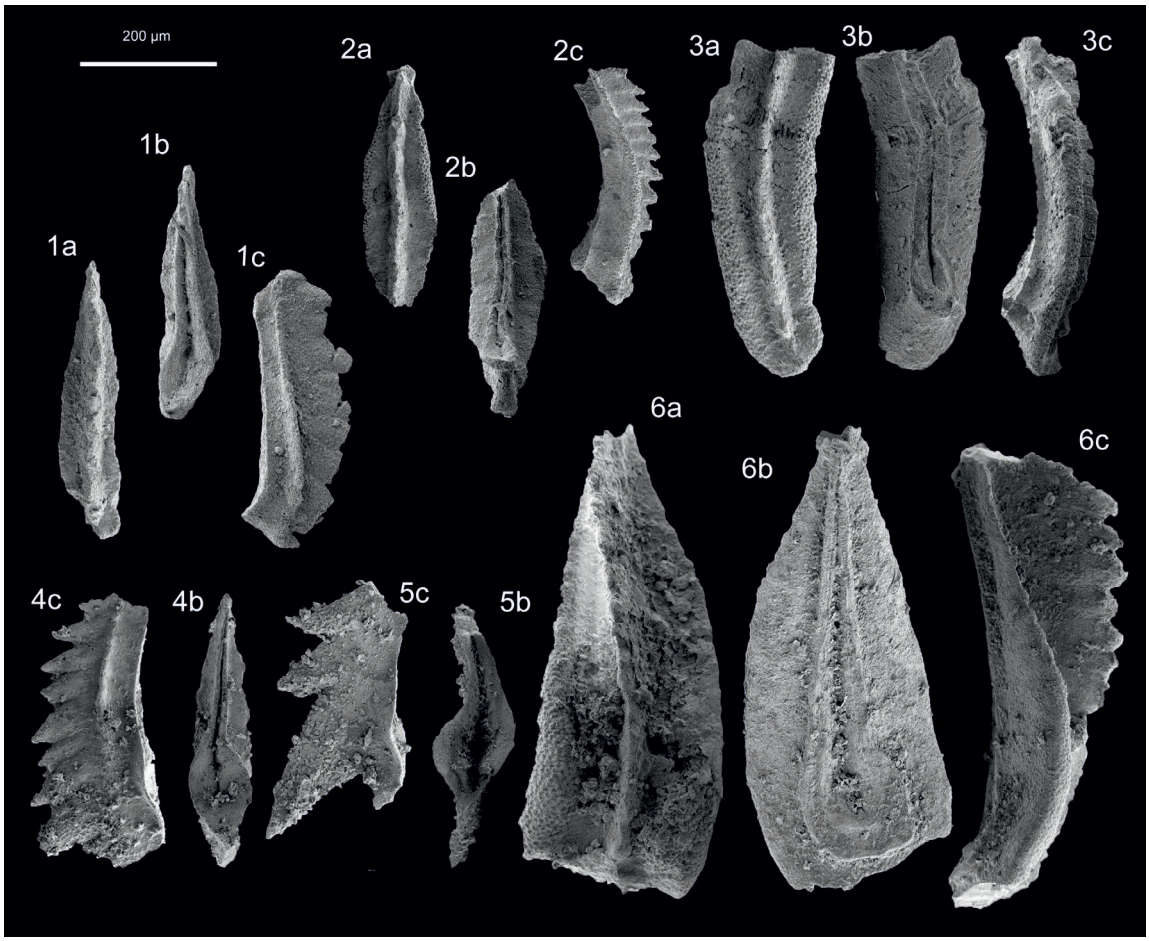

Fig. 5. Conodonts from the Ivanščica Mt. Column Preputnica: 1 – *Paragondolella eotrammeri* (Krystyn), sample PR-67.50; upper Illyrian–lower Fassanian. 2 – *Paragondolella trammeri* (Kozur), sample PR-67.50; upper Illyrian–lower Fassanian. 3 – *Neogondolella constricta* (Mosher and Clark), sample PR-67.50; upper Illyrian–lower Fassanian. Column Ivanečka Železnica II: 4 – *Budurovignathus* sp., sample IZ II-1.30; Ladinian. 5 – *Cratognathodus multihamatus* (Huckriede), sample IZ II-1.30; Ladinian. 6 – *Paragondolella* cf. *excelsa* Mosher, sample IZ II-1.30; Ladinian. a – upper, b – lower, c – lateral view. Scale: 200 microns. The illustrated conodont elements were photographed by the JEOL JSM 6490LV Scanning Electron Microscope at the Geological Survey of Slovenia (GeoZS), where the recovered materials are stored, inventoried and abbreviated GeoZS under the repository numbers 6326, 6333-6335, and 6338 in the micropaleontological collection.

while varieties with intersertal texture are occasional and visible only in the outer parts of the pillow (Fig. 4i). Phenocrysts (modal composition 20–50 vol.%) consist of unaltered to slightly albitised and sericitised subhedral to euhedral plate-like, alkali feldspar ($An_{0–6}Ab3_{–72}Or_{22–97}$) and plagioclase ($An_{3–64}Ab_{34–96}Or1_{–10}$), ranging in size from 0.5 to 5 mm (Fig. 4). The main ferromagnesian mineral is subhedral to anhedral clinopyroxene (up to 3 mm in size), whose composition corresponds to augite ($Wo_{39.8–44.7}En_{37.3–48.8}Fs_{7.3–22.9}$; Fig. 4d, e) with a wide range of Mg# (63–90) and Al^{VI}/Al^{IV} ratios (0.3–2.5). Clinopyroxene crystals are characterised by normal zoning, marked by a decrease in Mg# and Ca and an increase in Ti toward the rims, while reverse zoning is rarely observed. Spinel is a minor mineral phase (up to 0.5 mm in size) of homogeneous composition corresponding to Al-rich chromite (Fig. 6c). Magnesium and Cr numbers of spinel group are moderately high (Mg#=48, Cr#=52.7–56.6), as well as the content of FeO (up to 33.76 wt.%). Accessory minerals include apatite, zircon, and titanite. The most abundant secondary alteration phase is fine-grained, plate-like chlorite (trioctahedral Mg-chlorite (clinochlore), according to Zane & Weiss 1998; Fig. 6e). In contrast, Na–Ca amphibole (taramite; Fig. 6d) is quite rare in the studied volcanic rocks. Other phases are most commonly represented by bluish to greenish needle-like to fine-grained aggregate pumpellyite-(Fe^{2+}) (FeO=9.39–20.10 wt.%, Fe#=55.6–87.9; Fig. 6f) and often associated with needle-like to plate-like prehnite of stoichiometrically ideal composition (Supplementary Table S1). This mineral association is typical of ocean floor metamorphism. Secondary, fine-foliated muscovite, which is present in some samples, show a uniform chemical composition (Al_2O_3=29.46–31.15 wt.%, Na_2O=1.19–1.67 wt.%, K_2O=9.02–9.62 wt.%). Accessory titanite (grothite; Deer et al. 2013) is characterised by high Al and Fe (Supplementary Table S1). The microhypocrystalline matrix of the studied lavas is composed of partly devitrified volcanic glass, microlites of plagioclase, and

alkali feldspars (Fig. 4d–i). Our petrographic observations are consistent with the X-ray diffraction qualitative and quantitative analysis of the rocks presented in Šegvić et al. (2023a). The predominant alteration products are albite, chlorite, and quartz, while minor hydrothermal phases in some lava samples included amphibole, pumpellyite, prehnite, illite/smectite, and ilmenite.

Bulk-rock chemistry

Supplementary Table S2 shows the chemical composition of the analysed volcanic rocks. The silica and alkali contents vary over a wide range, as do the concentrations of the majority of other major element oxides, except for TiO_2 (0.77–1.48 wt.%) and P_2O_5 (0.13–0.31 wt.%). The loss on ignition value

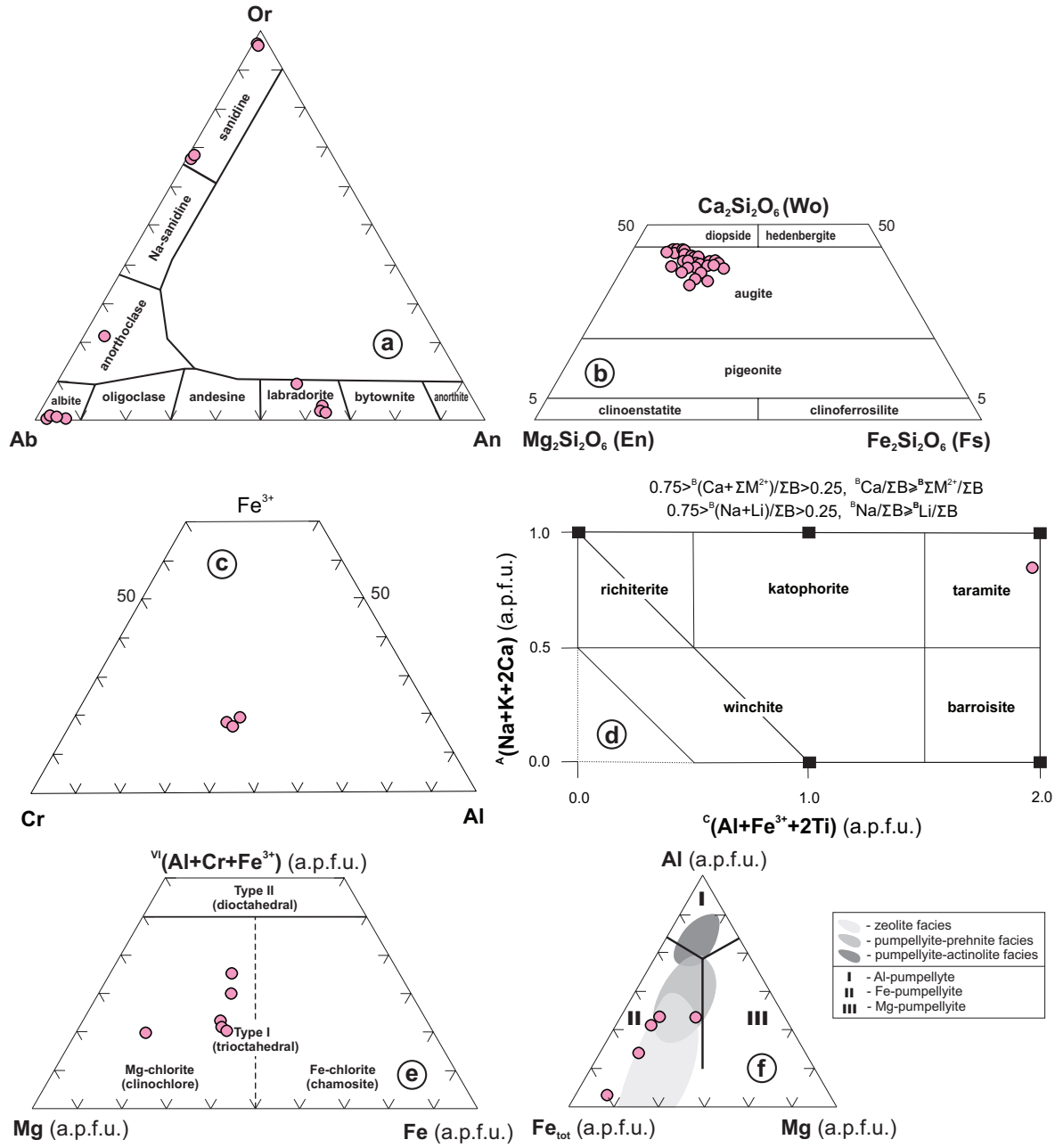

Fig. 6. Classification diagrams for **(a)** feldspar (Ab–An–Or plot; Deer et al. 1992; Dana et al. 1993), **(b)** pyroxene (En–Wo–Fs ($Mg_2Si_2O_6$–$Ca_2Si_2O_6$–$Fe_2Si_2O_6$) plot; Morimoto 1988), **(c)** spinel (trivalent Cr–Al–Fe^{3+} ternary cation plot), **(d)** amphibole (Al^{IV}–$(Na+K)^A$ plot; from Leake et al. 1997 and Hawthorne et al. 2012), **(e)** chlorite [Mg–Fe–$^{VI}(Al+Cr+Fe^{3+})$ plot; Zane & Weiss 1998] and **(f)** pumpellyite (Fe_{tot}–Mg–Al plot; Coombs et al. 1976) from the Middle Triassic calc-alkaline basaltic rocks from the Mt. Ivanščica. Compositional fields for pumpellyite from the East Taiwan Ophiolite basalts (zeolite facies), basalts from the Olympic Peninsula (prehnite–pumpellyite facies) and basalts from the Taveyannaz Formation (upper prehnite–pumpellyite and pumpellyite–actinolite facies) are taken from Coombs et al. (1976) and Rahn et al. (1994), respectively.

(LOI) also varies over a wide range and is generally moderately high (up to 5.9 wt.%). Therefore, we will carefully assess the mobility of oxides of major elements, trace elements, and rare earth elements (REE) by testing them in variation plots in which their concentrations are plotted against Zr content (Supplementary Fig. S1) as a differentiation index (e.g., Pearce 1975). On the variation diagrams, the majority of major element oxides and (to a lesser extent) the large ion lithophile elements (LILE; Cs, Rb, Ba, Sr), as well as transition metals (V, Cr, Ni) do not show any correlation with the differentiation index; therefore, they are not used for petrogenetic considerations. In contrast, high field strength elements (HFSE; Th, Nb, Ta, Hf, Y) and (to a lesser extent) REE and MgO show a good correlation with the differentiation index and thus can be considered suitable for further geochemical and petrogenetic interpretation (as has been successfully applied to similar rocks formed in different tectonic settings (e.g., Pearce & Norry 1979; Beccaluva et al. 1983)).

On the classification diagram Nb/Y vs. Zr/TiO_2*10^{-4} (Pearce 1996), analysed rocks fall in the field of sub-alkaline basalts, while only one sample corresponds to basaltic andesite (Fig. 7a). A wide range of moderately high Th/Yb (1.0–3.3) and Ta/Yb (0.1–0.2) ratios indicates their calc-alkaline to shoshonitic affinity (Fig. 7b). The studied lavas are characterised by a wide range of Mg# (33–70), Cr (11–348 ppm) and Zr (64–174 ppm). High Zr contents reflect an abundance of zircon.

In the primitive, mantle-normalised and multi-elemental plots (Fig. 8a), all rocks show significant LILE (Cs, Ba, Rb, K) and Th enrichment over a wide range from 7 to 600 times relative to the primitive mantle and a generally moderately inclined profile from La to Lu with decreasing abundance of less-incompatible elements ranging from 4 to 9 times relative to the primitive mantle. All samples show negative anomalies of Nb–Ta pair relative to La $[(Nb/La)_N=0.19–0.50]$, as well as of Ti $[(Ti/Gd)_N=0.33–0.83]$ and variable positive Pb spikes relative to Ce $[(Pb/Ce)_N=1.50–5.26]$. In contrast, Sr is characterised by a dominant, negative anomaly, while only the samples with the lowest Zr content show a weak positive anomaly $[(Sr/Nd)_N=0.10–1.86]$.

The chondrite-normalised REE patterns (Fig. 8b) show significant enrichment of light rare earth elements (LREE) over heavy rare earth elements (HREE) $[(La/Lu)_{CN}=3.01–7.39]$ at 29 to 84 times chondrite abundances, whereas the patterns of HREE are nearly flat $[(Tb/Lu)_{CN}=0.93–1.69]$ at 8 to 23 times relative to chondrite. A moderate negative Eu anomaly (Eu/Eu*=0.62–0.92) was observed in all samples.

Neodymium and Sr isotope compositions of representative basalts and andesite–basalt are shown in Supplementary Table S3 and Figure 9. The $^{143}Nd/^{144}Nd$ ratios are quite homogeneous, ranging from 0.512544 to 0.512655, while $^{87}Sr/^{86}Sr$ shows a wide range between 0.705633 and 0.720568. The initial ε_{Nd} and initial isotopic ratios for Sr are calculated for 243 Ma, which is the crystallization age of the analysed rocks (see below). The initial ε_{Nd} varies between −0.08 to +1.90, while the initial $^{87}Sr/^{86}Sr$ varies in a wide range from 0.704765 to 0.709248. The sample projection in the $\varepsilon_{Nd(t)}$ vs. $^{147}Sm/^{144}Nd$ diagram (Fig. 9b), located in the zone between subducted juvenile material (SJM), subducted continental material (SCM), and ocean island basalts (OIB) or depleted mantle (DM). This specific composition of the continental lithosphere influenced the composition of the magma and consequently the composition of the volcanic rocks that occur in the study area.

$^{40}Ar/^{39}Ar$ dating

The results of the $^{40}Ar/^{39}Ar$ experiments on a plagioclase separate from the andesite-basalt sample TSI-11 (Fig. 2a, location 7) are reported in Supplementary Table S4 and Figure 10. The heating steps 1–7 suggest an apparent age of 243±1.8 Ma.

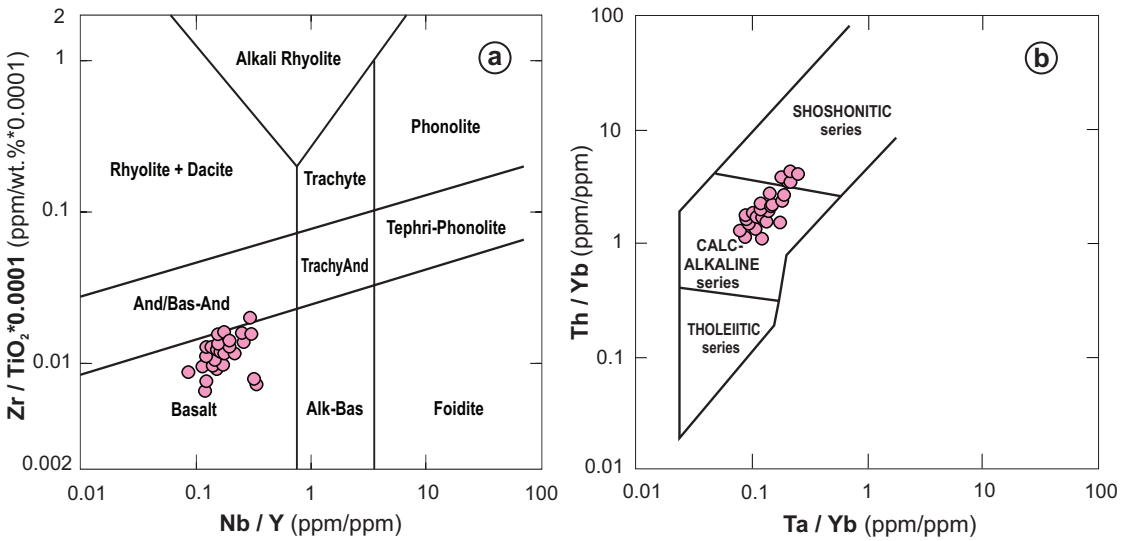

Fig. 7. (a) Nb/Y–Zr/TiO_2*10^{-4} classification diagram (Pearce 1996) and **(b)** Ta/Yb–Th/Yb discrimination diagram (Müller et al. 1992) for the Middle Triassic calc-alkaline basaltic rocks from the Ivanščica, Strahinjščica, Desinić Gora, and Olimska Gora Mts.

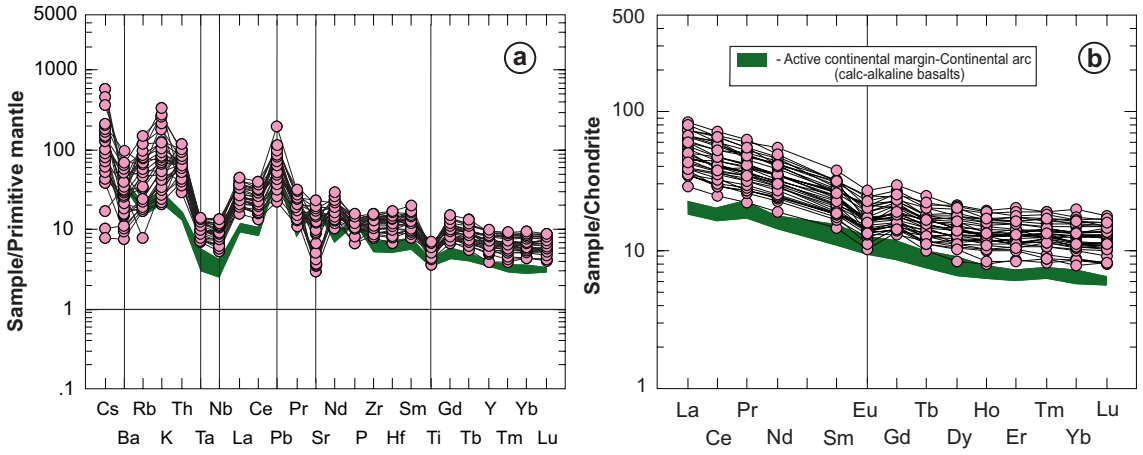

Fig. 8. (a) Primitive mantle-normalised multielement and **(b)** chondrite-normalised REE diagrams for the Middle Triassic calc-alkaline basaltic rocks from the Ivanščica, Strahinjščica, Desinić Gora, and Olimska Gora Mts. Normalisation values are from Sun & McDonough (1989). Patterns for average primitive calc-alkaline basalt from active continental margin-continental arc (Schmidt & Jagoutz 2017) are plotted for correlation constrains.

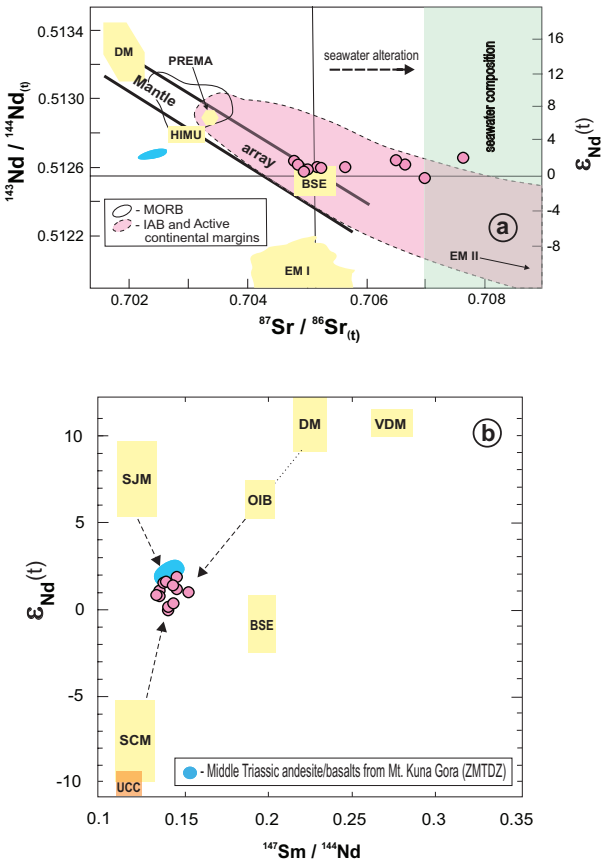

Fig. 9. (a) Initial $^{143}Nd/^{144}Nd$–$^{87}Sr/^{86}Sr$ isotope ratios diagram for the Ivanščica and Strahinjščica Mts. Middle Triassic calc-alkaline basaltic rocks showing the main oceanic mantle reservoirs of Zindler & Hart (1986). DM=depleted mantle, BSE=bulk silicate Earth, EMI and EMI II=enriched mantle, HIMU=mantle with high U/Pb ratio, PREMA=PREvalent MAntle composition. Data for mid-ocean ridge basalts – MORB compiled from Wilson (1989) and references therein and Cousens et al. (1994), references therein and Peate et al. (1997). Data for oceanic island arcs and active continental margins – IAB compiled from Wilson (1989) and references therein, Cousens et al. (1994) and references therein, Pearce et al. (1995) and Peate et al. (1997). The field for $^{87}Sr/^{86}Sr$ values affected by syn- or post-magmatic alteration in contact with seawater (light-green shading) is from Ustaszewski et al. (2009). **(b)** $^{147}Sm/^{144}Nd$–$\varepsilon_{Nd(t)}$ isotope ratios diagram for the Middle Triassic calc-alkaline basaltic rocks from the Ivanščica and Strahinjščica Mts. Hypothetical mantle sources: DM=depleted mantle (not refractory), VDM=very depleted mantle (refractory), SJM=subducted juvenile material (subducted oceanic crust; slab with little pelagic sediment), SCM=subducted continental material and BE=bulk earth. The observed compositions and hypothetical end members sources calculated for the Middle Triassic following Swinden et al. (1990). Fields for Kuna Gora Mt. calc-alkaline andesite–basalt (Slovenec & Šegvić 2021) are plotted for comparison.

On the geological time scale (Ogg et al. 2016; Gradstein et al. 2020), this age corresponds to the Middle Triassic (Late Anisian; Pelsonian–Illyrian) and is interpreted as the age of basalt eruption. This age is very similar to the isotopic ages of high-K calc-alkaline basaltic lavas of Kuna Gora Mt. (241.1±5.2 Ma; Slovenec & Šegvić 2021) and basic pyroclastic rocks of the central part of Ivanščica Mt. (244.5±2.8 Myr; Smirčić et al. 2024). Each of these isotopic ages of lavas and pyroclastics, along with the paleontological ages of sediments interstratified with them, indicate short (~3–4 Ma) effusive volcanic activity in the NCTRB during the Middle Triassic (Bithynian–Fassanian).

Discussion

Brief lithostratigraphic interpretation of volcano-sedimentary successions

The Middle Triassic volcano-sedimentary successions of northwestern Croatia were interpreted as deposited in a tectonically active environment with deposition controlled by intense tectonics and volcanism (Goričan et al. 2005; Slovenec

et al. 2020, 2023a; Kukoč et al. 2023; Smirčić et al. 2024). Rift-related extension, which led to the opening of the Neotethys Ocean in the Middle Triassic (Kukoč et al. 2024; Slovenec & Šegvić 2024 and references therein), created a complex topography of grabens and half-grabens in which pelagic sediments and volcaniclastic detritus accumulated. Rapid deepening along steep normal faults resulted in the redeposition of material from lateral areas with still active, shallow-marine carbonate production (Goričan et al. 2005; Kukoč et al. 2023). These steep normal faults also likely served as conduits for basaltic to andesite-basaltic magma to reach the surface (Slovenec & Šegvić 2021; Kukoč et al. 2023; Smirčić et al. 2024). At the same time, the rhyolitic "Pietra Verde" tuffs were deposited in these environments as pyroclastic density currents and as air-fall deposits (Kukoč et al. 2023; Slovenec et al. 2023a; Smirčić et al. 2024). Such pyroclastic rocks were prone to reworking, redistribution, and mixing with pelagic sediments (limestones or cherts). With the main Neotethyan rift located further to the east, extension in the research area ceased in the Ladinian, resulting in the infilling of pelagic areas and the reestablishment of shallow-marine carbonate sedimentation (Kukoč et al. 2023). The stratigraphic position of volcanic and pyroclastic rocks within these successions (Fig. 3) indicates that the volcanic activity that produced effusive basic/intermediate lithologies preceded explosive volcanic eruptions which produced rhyolitic "Pietra Verde" tuffs (Kukoč et al. 2023; Slovenec et al. 2023a), although coeval bimodal volcanism has also been previously suggested (Fig. 3; Smirčić et al. 2024).

Petrogenesis of volcanic rocks

The studied basaltic and andesite–basaltic rocks were formed in submarine condition, as indicated by their appearance in the form of pillow lavas (Fig. 4c). The primary crystallisation sequence (spinel → clinopyroxene → plagioclase → alkali feldspar ± Fe–Ti oxides) of these lavas is typical for basaltic and andesite–basaltic rocks. However, the presence of secondary mineral phases (albite, chlorite, prehnite, pumpellyite and Na–Ca amphibole), devitrified volcanic glass (to a lesser extent), as well as moderate chemical variation (mobilisation) of the majority of oxides of major elements, LOI, LILE, and some transition metals (Supplementary Fig. S1 and Supplementary Table S1) in part of the samples indicate post-magmatic alteration processes by which the lavas were affected. In this sense, Na–Ca amphibole (taramite; Fig. 6d) is formed by alteration of pyroxene with the introduction of Na from plagioclase under conditions that correspond to a higher stage of the greenschist facies during oceanic crust metamorphism, similar to metabasalts of the Rakovec Group (SE Slovakia) in the Gemeric Unit (Faryad & Bernhardt 1996). This could indicate an aborted recycled Paleotethys. However, the formation of albite, followed by prehnite and pumpellyite associated with the albitisation of plagioclase, which supplies the Al required for their crystallisation (Deer et al. 2013), indicates submarine deuteric alteration and subsequent low-grade

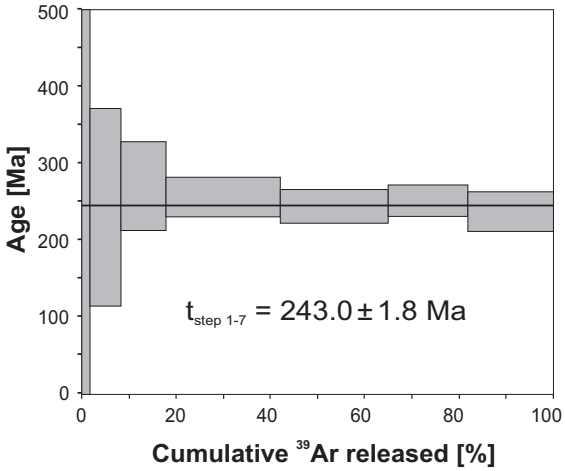

Fig. 10. Results of the $^{40}Ar/^{39}Ar$ step heating experiment on separated plagioclase crystals from sample TSI-11(Mt. Ivanščica).

metamorphism within the prehnite–pumpellyite facies. Somewhat lower alteration conditions are suggested by Mg-rich chlorite (clinochlore; Fig. 6e), which is the dominant secondary phase in the studied rocks. Chlorite geothermometry yields temperatures between 120 °C and 200 °C (Cathelineau 1988; Jowet 1991; Inoue et al. 2018). These values likely reflect the temperature of chlorite crystallisation during late hydrothermal alteration (Vidal et al. 2005, 2016; Šegvić et al. 2023a) rather than the peak metamorphic conditions of the assemblage, which are constrained by the occurrence of prehnite and pumpellyite. Evidence for locally, higher-temperature, seafloor hydrothermal alteration is provided by devitrified volcanic glass preserved within the micro-hypocrystalline matrix (e.g., Tillick et al. 2001; Wang et al. 2018). Post-depositional alteration processes most likely influenced the variability of silica content as well, whose high concentrations (Supplementary Table S2) have no clear footing in the petrographic observations, but suggest its mobility.

Dominant normal zoning, with rarely observed reverse zoning of primary clinopyroxene crystals, may indicate the dominance of a closed crystallisation system compatible with calc-alkaline magmatic series. The maximum crystallisation temperatures and pressures of the clinopyroxene, which are in equilibrium in the rock (Fig. 4j), range from 1023 °C to 1090 °C and 0.3 to 0.5 GPa (according to the Chicchi 2023 geothermobarometer; cpx-only) and 1050 °C to 1085 °C (according to the Neave & Putirka 2017 geothermobarometer; cpx-liquid pairs), with estimated pressures ranging from 0.3 to 0.6 GPa. Slightly higher equilibration pressures of clinopyroxene, ranging from 0.4 to 0.9 (±0.2) GPa, are indicated by the geobarometers based on the findings of Nimis (1999) and Nimis & Ulmer (1998). These conditions correspond to a magma storage depth of approximately 33 km.

Careful and detailed analysis of HFSE and REE (Supplementary Fig. S1 and Supplementary Table S2) showed that these elements remained immobile, i.e., that they retained the primary magmatic features. Therefore, petrogenetic considera-

tions are based on the distribution of HFSE and REE, as well as their discrimination ratios and Nd isotopic data. The genesis of the studied calc-alkaline/shoshonitic lavas can be linked to the contamination of subduction-generated magma by lithospheric mantle melts or mantle sources that were enriched by subduction-related crustal melts. This is indicated by Th and LREE enrichments (Fig. 8a, b) while the negative anomalies of Nb–Ta pair relative to La [$(Nb/La)_N$=0.19–0.50; Fig. 8a], reflect partial melting of a depleted mantle source (the supra-subduction mantle wedge). Low Sm/La (0.22–0.33), together with high Th/La (0.19–0.49) typical of subduction-related melts, likely derived from crustal material (Fig. 11). The negative Ti anomaly [$(Ti/Gd)_N$=0.33–0.83] in all samples may also suggest the influence of a depleted mantle, i.e. the generation of magma by melting of a (subduction-modified) metasomatised mantle (e.g., Pearce et al. 1984; Hofmann 1997), while in samples where magnetite is registered, it may also indicate its fractionation. However, the chemical composition of volcanic rocks may also be a consequence of the specific composition of the subcontinental lithosphere (Hooper et al. 1995). The low $\varepsilon_{Nd(t)}$ values (between −0.08 and +1.90), which is slightly above those for the Bulk Silicate Earth, and low $^{147}Sm/^{144}Nd$ ratios (≤0.152061; Supplementary Table S3) (Fig. 9a, b), as well as positive Pb spikes (up to 5.3; Fig. 8a), indicate a low influence of subducted continental crust in the genesis of the investigated basaltic lavas. However, the sample projection in the $\varepsilon_{Nd(t)}$ vs. $^{147}Sm/^{144}Nd$ diagram (Fig. 9b), located in the zone between subducted juvenile material (SJM), subducted continental material (SCM), and depleted mantle (DM) or ocean island basalts (OIB), clearly suggests interaction and mixing of magmas from multiple source regions. It can be assumed that the dominant role was played by subducted juvenile material (SJM), likely originating from the previous subducted oceanic crust of the Paleotethys, which was then a somewhat subordinate subducted continental material (SCM), i.e., sediments recycled in the mantle wedge, while the presence of DM- or OIB-like mantle material was negligible (Fig. 9b). This corresponds to the already commented/elaborated geochemical features shown in Figs. 7 and 10. At the same time, although the analysed samples show a wide range of initial $^{87}Sr/^{86}Sr$ ratios (Fig. 9a), the majority still have mantle-array characteristics, while high values in some samples indicate ocean-floor hydrothermal metamorphism, i.e., significant seawater alteration (e.g., Bach et al. 2003).

The possible mantle sources of the studied Middle Triassic lavas and the degree of partial melting can be investigated using the petrogenetic model based on the Dy/Yb vs. Yb relationship (Fig. 12). Only samples with the highest Mg# and MgO content (Mg#=70.4–56.3; MgO=8.45–6.25 wt.%) were used for modeling, presenting either a primitive or near-primitive composition of the melt. According to this partial melting model, the analysed rocks plot along a melting curve representing a spinel mantle source region, and the degree of partial melting ranges from 5 % to 14 %. This wide range of spinel source partial melting degrees reflects a relatively shallow mantle source region. This is also supported by the absence of

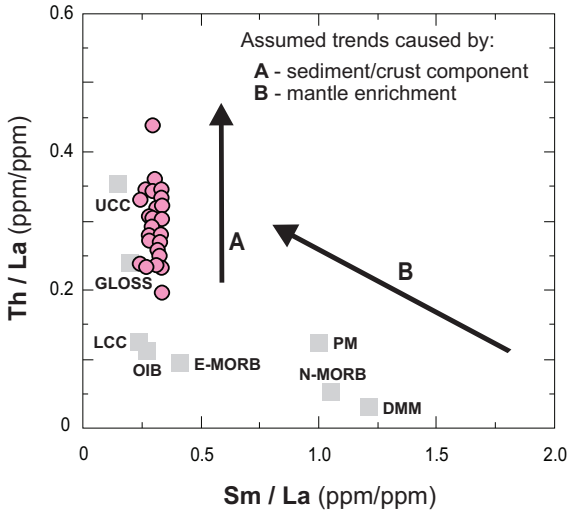

Fig. 11. Th/La–Sm/La diagram for the Middle Triassic calc-alkaline basaltic rocks from the Ivanščica, Strahinjščica, Desinić Gora, and Olimska Gora Mts. (from Plank 2005). Abbreviations: [N-MORB=normal mid-ocean ridge basalts; E-MORB=enriched MORB; OIB=ocean island basalts; PM=primitive mantle (Sun & McDonough 1989)]; [UCC=upper continental crust; LCC=lower continental crust (Taylor & McLenann 1985)]; GLOSS=global subduction sediment (Plank & Langmuir 1998); DMM=depleted MORB mantle (Workman & Hart 2005).

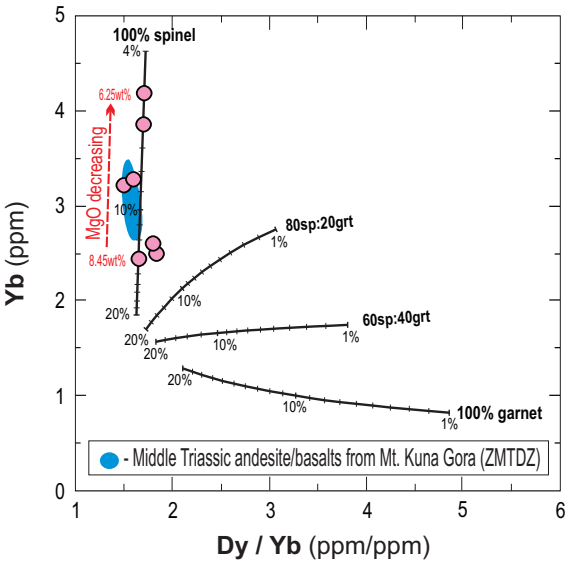

Fig. 12. Yb–Dy/Yb diagram for the most primitive Middle Triassic calc-alkaline basaltic rocks samples from the Ivanščica, Strahinjščica, Desinić Gora, and Olimska Gora Mts. Partial melting curves are shown for the non-modal batch melting of spinel and garnet lherzolite sources, starting from a Primitive Mantle (PM; McDonough & Frey 1989) material. Mineral and melt modes for spinel and garnet–lherzolite source: $Ol_{0.53(0.10)} + Opx_{0.27(0.27)} + Cpx_{0.17(0.50)} + Sp_{0.03(0.13)}$ (Kinzler 1997) and $Ol_{0.60(0.05)} + Opx_{0.21(0.20)} + Cpx_{0.08(0.30)} + Gt_{0.12(0.45)}$ (Walter 1998), respectively. Italic numbers in parentheses indicate the percentages of each mineral entering the liquid. Partition coefficients are from McKenzie & O'Nions (1991). Fields for Kuna Gora Mt. calc-alkaline andesite-basalt (Slovenec & Šegvić 2021) are plotted for comparison.

HREE depletation (Yb_{CN}>10), which indicates the absence of garnet in the source and melting at low pressure (Fig. 8b).

In addition to partial melting, the formation of the investigated rocks involved fractional crystallisation [$(La/Lu)_{CN}$= 3.01–7.39] after segregation from their source region. The fractionation of key liquidus phases controlling the melt composition (plagioclase and alkali feldspar) is indicated by the prominent negative anomalies of Eu (Fig. 8b), while clinopyroxene fractionation is reflected in the negative linear trend of the Sc/Yb ratio with decreasing Mg# (Kamenetski et al. 2000; Supplementary Fig. S2).

In conclusion, we suggest that the formation of the magmas from which the studied Middle Triassic calc-alkaline/shoshonitic lavas are derived is the result of the process of partial melting of metasomatised subcontinental lithospheric mantle contaminated by components, most likely inherited from a previously subducted lithosphere and the process of subsequent fractional crystallisation. The formation of these magmas could have taken place at or near the mantle-crust transition (in which the MASH process usually occurs) in the area above subduction zones, as well as those below long-lived intraplate volcanoes (Hildreth & Moorbath 1988), similar to the Middle Triassic basalts of the nearby Kuna Gora Mountain (Figs. 9b and 12; Slovenec & Šegvić 2021). Furthermore, the abundance of post-magmatic secondary deuteric phases primarily consists of chlorite and albite, along with minor amounts of prehnite, pumpellyite, epidote, amphibole, mica, and intermediate swelling clays. This is consistent with ocean-floor hydrothermal metamorphism that impacted the active Neotethyan continental margin (Alt & Teagle 2000; Šegvić et al. 2023a). Based on the documented paragenetic assemblages, low to medium degrees of metamorphism are inferred, extending from prehnite–pumpellyite to lower greenschist facies conditions.

Tectonomagmatic and geodynamic significance

It is generally recognised that calc-alkaline volcanic rocks are typical products of magmas generated at convergent destructive plate margins, which are usually associated with subduction zone settings, such as continental and island arcs (e.g., Gill 1981), but their chemistry may also be a consequence of the specific composition of the subcontinental lithosphere (Hooper et al. 1995). However, due to the interaction of different magma reservoirs, which are recycled within the mantle wedge, magma genesis becomes highly complex, leading to the formation of magmatic rocks with contrasting petrological characteristics at convergent destructive plate margins (e.g., Pearce 1983; Arculus & Powell 1986; Hawkesworth et al. 1991; Plank 2005). Given that the magma from which the investigated volcanic rocks were derived had a complex evolution, it is not straightforward to unravel the tectonomagmatic provenance of the studied basalt suite. Key indicators include: (a) negative anomalies in Nb–Ta and Ti (Fig. 8a) mainly suggest partial melting of depleted mantle (Pearce 1982, 1983; Arculus & Powel 1986; Hawkesworth et al. 1993; Wang et al. 2016), (b) enrichment in Th (Fig. 8a), (c) downward patterns from LREE to HREE in the chondrite-normalised REE diagram (Fig. 8b), as well as isotopic data (Fig. 9a, b), suggest formation in a subduction-related environment associated with an ensialic volcanic arc developed in an active continental margin setting. Supporting this are the projections of the analysed rock in the discrimination diagrams Hf/3–Th–Nb/16, Th_N–Nb_N and Th/Nb vs. La/Yb (Fig. 13a–c) within the orogenic field (convergent tectonic settings), which is typical of a calc-alkaline volcanic arc or active continental margin-related volcanic suites. However, these geochemical features, which are most likely inherited from older (Hercynian), arc-related lithologies associated with the Paleotethys subduction (Slovenec & Šegvić 2021) and reflect mantle metasomatism related to an older (ancient) event of subduction, may therefore not accurately define the tectonic context at the time of the emplacement of the studied rocks. This is supported by the chemistry of the primary magmatic ferromagnesian phase (clinopyroxene) from the analysed basalt, which connects their origin with the processes of continental crust rifting (Fig. 13d).

Therefore, the geodynamic evolution of the investigated Middle Triassic basaltic suite, which crops out in the mountains of northwest Croatia and northeast Slovenia, in the northernmost segment of the Dinarides (Fig. 1a, b), could be linked to: (i) a subduction geotectonic model coeval with an active, ensialic volcanic arc, but also to (ii) a model of formation in a rift-related environment. Bearing in mind the complexity of the geotectonic setting of the investigated lavas, as well as the absence of clear geological evidence, it is not possible to propose a definitive geodynamic model of their origin. Therefore, we propose two alternative models based on different paleogeographic reconstructions to shed light on the origin of the studied rocks. The first model, which is based on the paleogeographic reconstruction proposed by Stampfli & Borel (2002, 2004) and Stampfli & Hochard (2009) (Fig. 14a1) favors the active northward subduction of the Paleotethyan lithosphere beneath Laurasia (Eurasian Plate) during the Middle Triassic, coupled with wet melting in the mantle wedge (Fig. 14a2). The final closure of this ocean realm occurred in the Late Triassic. According to this model, the investigated calc-alkaline/shoshonitic continental arc-related volcanism of the active continental margin is the result of active subduction and associated partial melting of the sublithospheric mantle. In this context, subduction events during the Late Paleozoic (Pe-Piper 1998) played an important role in hydrating the subcontinental lithospheric mantle. Consequently, active subduction could have released some fluids which thus lowered the solidus of the mantle wedge, thereby permitting its melting. The second model, which is based on a more recently proposed paleogeographic reconstruction by van Hinsbergen et al. (2020) and van Hinsbergen & Schouten (2021) (Fig. 14b1), links the Middle Triassic opening of the Balkan Neotethys Ocean during the early break-up of Pangea to a southwestward subduction of the Balkan Paleotethyan lithosphere beneath the northeastern Greater Adria–Dacia margin, followed by the rollback of the Balkan Paleotethys slab (Fig. 14b2). Unlike

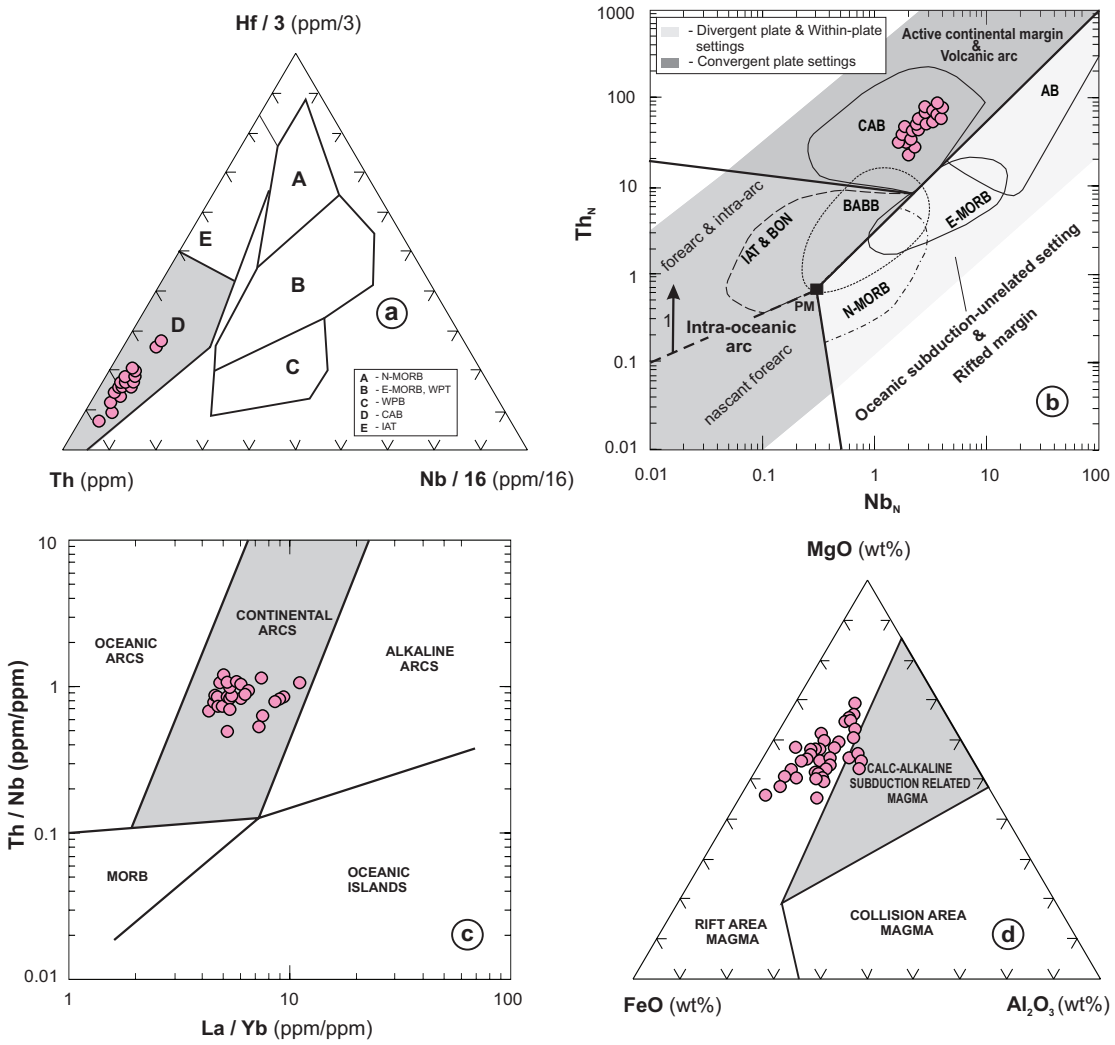

Fig. 13. Discrimination diagrams for the Middle Triassic calc-alkaline basaltic rocks from the Ivanščica, Strahinjščica, Desinić Gora and Olimska Gora Mts. **(a)** Th–Nb/16–Hf/3 diagram (Wood 1980). Abbreviations: A=normal mid-ocean ridge basalts (N-MORB); B=enriched MORB (E-MORB) and within-plate tholeiites (WPT); C=alkaline within-plate basalts (AWPB); D=calc-alkali basalts (CAB); E=island-arc tholeiites (IAT). **(b)** Th_N–Nb_N diagram (Saccani 2015). Th and Nb normalised to the N-MORB composition (Sun & McDonough 1989). Abbreviations: AB=alkali basalts, BABB=back-arc basin basalts, BON=boninites, CAB=calc-alkali basalts, IAT=island-arc tholeiites, N-MORB=normal mid-ocean ridge basalts, E-MORB=enriched MORB, PM=primitive mantle. **(c)** La/Yb–Th/Nb diagram (Hollocher et al. 2012). **(d)** FeO–Al_2O_3–MgO diagram (Le Bas 1962) for pyroxene.

the first model, this one excludes the influence, i.e., the effect of active subduction during the formation of the investigated calc-alkaline/shoshonitic basaltic suite due to the already significant subducted plate retreat, i.e., a highly advanced slab rollback process and favors extensional lithospheric events associated with passive continental rifting along the mid-Triassic margins of Greater Adria. In this regard, the rifting area where volcanism was generated was already quite distant from the trench at that time (Fig. 14b2). The formation of calc-alkaline/shoshonitic basaltic suite in this context involved rift-related: (i) partial melting of the heterogeneous subcontinental lithospheric mantle, where the isothermal relaxation allowed the previously metasomatised sources to melt and (ii) crustal contamination, i.e., recycling of the mantle source. These metasomatised sources were contaminated by components most likely inherited from earlier Hercynian subduction events in the Late Paleozoic (*sensu* Saccani et al. 2015).

Ultimately, this effusive volcanism, as outlined through both proposed geodynamic models, produced predominantly submarine basaltic lava, which was ejected/erupted to the surface along tectonically weakened zones of the crust (Fig. 14a2 and b2). On the surface, basaltic lavas were interstratified with deep-sea siliciclastic and carbonate sediments (Fig. 3) during the Middle Triassic (Middle Anisian–Early Ladinian), forming a multiphase sequence within an intracontinental simple or half-graben syn-rift basin – the Northwestern Croatian Triassic Rift Basin (NCTRB; *sensu* Kukoč et al. 2023; Fig. 14a2 and b2). However, the development of the NCTRB, formed on

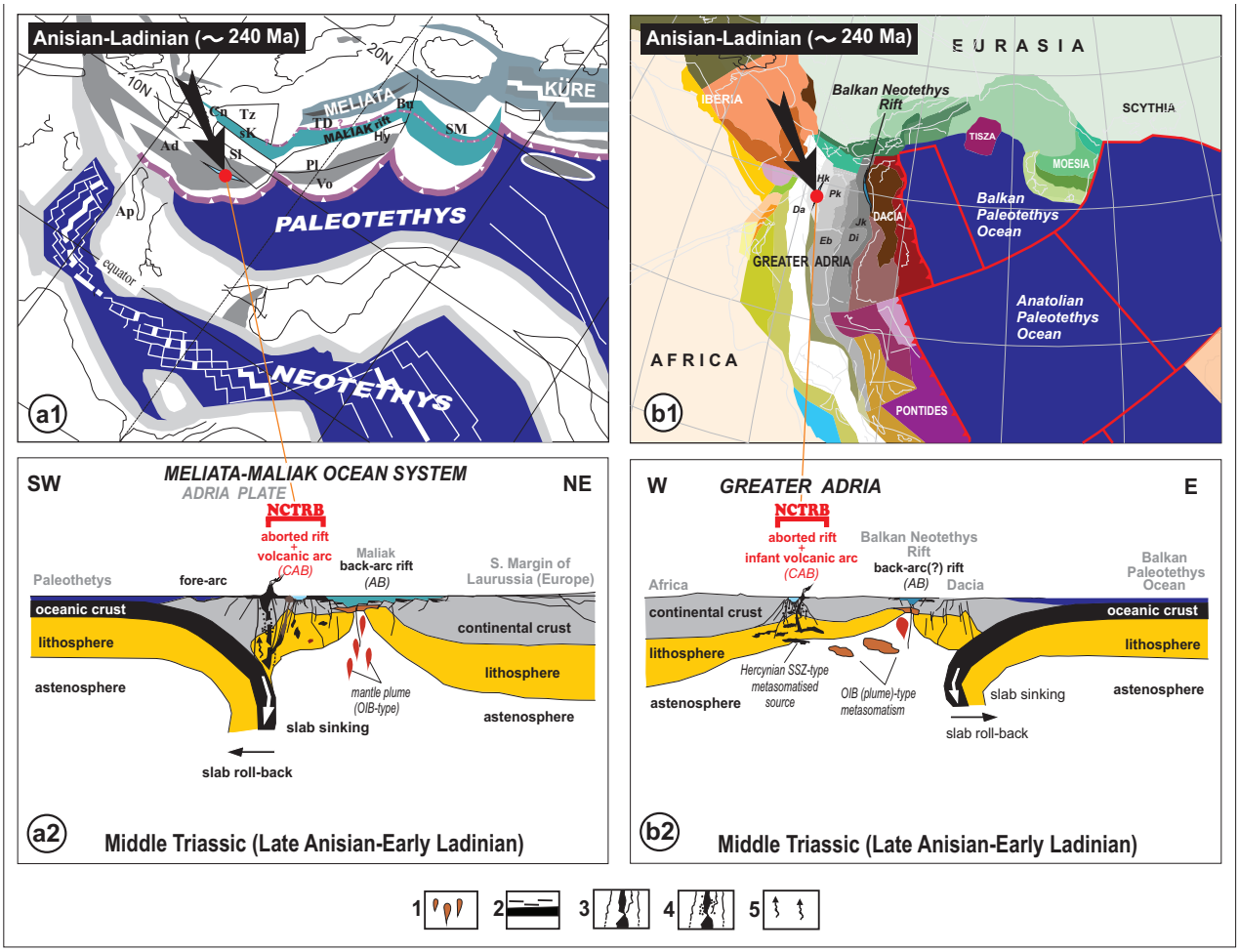

Fig. 14. Middle Triassic paleogeographic reconstruction of the Mediterranean region at Anisian-Ladinian times (~240 Myr): **(a1)** simplified after Stampfli & Borel (2004) [Ad=Adria Plate s. str., Ap=Apulia s. str., Bü=Bükk, Cn=Carnic-Julian, Hy=Hydra, Pl=Pelagonian, sK=south-Karawanken fore arc, Sl=Slavonia, SM=Serbo-Macedonian, TD=Trans-Danubian, Tz=Tisza, Vo=Vourinos (Pindos)] and the second north Balkan subduction zone introduced by Neubauer et al. (2019) and Spahić (2024); **(b1)** simplified and slightly modified after van Hinsbergen et al. (2020) [Da=Dalmatian Nappe, Di=Drina-Ivanjica Nappe, Eb=East Bosnian-Durmitor Nappe, Hk=High karst, Jk=Jadar-Kopaonik Nappe, Pk=Pre-Karst Nappe] with location of investigation area (marked with black arrow and red dot symbol). Schematic geodynamic model (scale is approximate) for: **(a2)** interaction of active continental margin magmatic activity (subduction-related ensialic volcanic arc magmatism) and roughly contemporaneous proto back-arc rifting [slightly modified from Slovenec & Šegvić 2024] according to Stampfli & Borel (2004) paleogeographic reconstruction shown in a1. **(b2)** Ensialic infant arc–back-arc rifting in the central part of the Mediterranean region according to van Hinsbergen et al. (2020) paleogeographic reconstruction shown in b1. Abbreviations: NCTRB=Northwestern Croatian Triassic Rift Basin; CAB=calc-alkaline and shoshonitic basalts, AB=alkaline basalts, OIB=ocean island basalts; 1=mantle diapires, 2=oceanic crust topped by radiolarian cherts, 3=partially melted, previously subducted oceanic lithosphere, 4=zone of partial melting and contamination by continental crust, 5=fluids from a previously subducted slab.

the edge of the Adria Plate (Greater Adria), resulted from the interplay of extensional processes, plate disintegration, and subsidence, and lasted for a remarkably short time (~3–4 Myr; Kukoč et al. 2023) until the Late Ladinian. Due to changes in regional geotectonic events during the Middle to Late Triassic, this basin was soon closed and therefore could not develop into an "classical" oceanic basin; instead, it formed as a locally aborted back-arc rift system of the Paleotethys (Slovenec & Šegvić 2024). The brief but highly intense bimodal effusive-explosive volcanic activity in the NCTRB, occurring over several volcanic events (Fig. 3), included not only calc-alkaline/shoshonitic basic dominant lavas and subordinate basic pyroclastic rocks (Smirčić et al. 2024), but also rhyolitic lavas and pyroclastic material (*Pietra Verde* tuffs; Slovenec et al. 2023a). Although formed over a very short period, the volcano-sedimentary successions uncovered in the NCTRB are characterised by a thickness exceeding 100 m (Fig. 3; Kukoč et al. 2023), thereby indicating intense and highly productive volcanic activity. With the closure of this basin, bimodal volcanic activity and the production of lava, as well as the associated pyroclastics, gradually diminished and ultimately ceased by the Late Triassic.

However, as early as the Late Anisian, there was a local passive upwelling of asthenospheric mantle, i.e., the uplift of

a primitive mantle dome due to adiabatic decompression along a system of subparallel faults (Slovenec et al. 2020), lateral to the NCTRB toward the southern margin of Laurussia (Europe; Fig. 14a2) and the Balkan Paleotethys Ocean (Fig. 14b2). The result of these events was proto-back-arc rifting of the intracontinental lithosphere behind the pericontinental, infant volcanic arc (Fig. 14a2 and b2; Slovenec et al. 2011). This rifting allowed melting of the primitive asthenospheric mantle and the formation of the magma from which alkaline (OIB-type) basaltic lavas free of crustal contamination were derived (Slovenec & Šegvić 2024 and references therein). Although contemporaneous with the studied calc-alkaline/shoshonitic volcanic rocks from the NCTRB, these alkaline basaltic lavas are not genetically related to them. Unlike the short-lived volcanic activity of the aborted NCTRB rift, magmatic activity in the Maliak back-arc rift (Fig. 14a2) or Balkan Neotethys Rift (Fig. 14b2) continued and progressed during the Late Triassic–Middle Jurassic period, eventually leading to the initial drifting and spreading of an ensialic back-arc basin (Slovenec et al. 2010, 2011), forming the northwestern segment of the Neotethyan oceanic system (see fig. 9 in Slovenec & Šegvić 2024).

In geodynamic and petrogenetic terms, the investigated Middle Triassic calc-alkaline/shoshonitic basic volcanic rock series, located in the northernmost segment of the Dinarides (Fig. 1a, b), can be correlated with equivalent rock suites in the Dinarides (Bébien et al. 1978; Pamić 1984; Trubelja et al. 2004; Pamić & Balen 2005; Radulović et al. 2014; Smirčić et al. 2018, 2020; Slovenec et al. 2023b), the Hellenides and Albanides (Pe-Piper & Panagos 1989; Pe-Piper & Mavronichi 1990; Capedri et al. 1997; Pe-Piper 1998; Monjoie et al. 2008; Chiari et al. 2012), as well as those from the Southern Alps and the Trans-Danubian region (Castellarin et al. 1980, 1988; Obenholzner 1991; Bonadiman et al. 1994; Harangi et al. 1996; Lustrino et al. 2019; De Min et al. 2020). However, in Bosnia-Herzegovina, Montenegro and Serbia, porphyrites and andesites also appear frequently. They are commonly associated with porphyry keratophyres in which Zn–Pb mineralization occurs (Brskovo, Šuplja Stijena, Crnac). Their appearance is not characteristically related to basalts, but to the beginning of rifting during the Middle Triassic. In this sense, the studied basic volcanic rocks from the NCTRB and equivalent rock suites from the aforementioned surrounding areas were formed in a similar geotectonic setting, and are characterised by a similar sequence of magma-genetic processes during their formation.

Conclusions

- The Middle Triassic multiphase effusive volcanic activity, accompanied by the sedimentation of shallow to deep marine carbonates, fine-grained clastic sedimentary rocks, and cherts, was deposited in an intracontinental simple or half-graben syn-rift basin (the Northwestern Croatian Triassic Rift Basin) located in the northernmost segment of the Dinarides. This period of volcanic and sedimentary activity was very brief, lasting approximately ~3–4 Myr (Middle Anisian–Early Ladinian, i.e., Bithynian–Fassanian).
- Basic massive and pillow lavas are represented by calc-alkaline/shoshonitic porphyritic/glomeroporphyritic basalt.
- The petrographic evidence indicates the following crystallisation sequence: spinel (Al-chromite) → clinopyroxene (augite; $Wo_{39.8–44.7}En_{37.3–48.8}Fs_{7.3–22.9}$) → plagioclase ($An_{3.2–63.6}Ab_{33.6–96.2}Or_{0.6–9.8}$) → alkali-feldspar ($An_{0.1–5.8}Ab_{2.5–72.4}Or_{21.8–97.4}$) ± Fe–Ti oxides with approximately the same modal proportion of high-temperature mafic ferromagnesian minerals (i.e., clinopyroxene) and low-temperature felsic mineral phases (i.e., feldspar).
- The microcrystalline matrix of the lavas consists of devitrified glass and microlites of plagioclase/alkali feldspar.
- The alteration products of ocean-floor hydrothermal metamorphism, represented by a series of Mg-chlorite, prehnite, Fe-pumpellyite and Na–Ca amphibole (taramite), define conditions of very low to low-grade metamorphism (prehnite–pumpellyite to higher-grade greenschist facies).
- Basaltic to andesite-basaltic lavas were formed through: (i) low-degree partial melting (5–14 %) of a shallow (spinel stability facies; max. depth ~33 km and max. pressures ≤0.9±0.2 GPa) magma source in the subcontinental lithospheric mantle and (ii) fractional crystallization in a partially open magmatic system.
- The magma was generated by the mixing of: (i) melts from the subducted slab – likely linked to the previously subducted oceanic crust of Paleotethys, (ii) less abundant previously subducted continental crustal material – sediments recycled in the mantle wedge, and (iii) a negligible contribution from DM- or OIB-like mantle. Melts from subducted slab and recycled sediments are most likely inherited from an earlier (ancient) subducted lithosphere during Hercynian subduction events (likely in the Late Paleozoic).
- The complex geodynamic evolution of the Middle Triassic basaltic lavas archived in the NCTRB (locally aborted back-arc rift systems of the Paleotethys), can be explained by two alternative models: (i) the subduction of the Paleotethyan lithosphere associated with an ensialic volcanic arc developed in an active continental margin setting, and (ii) the processes of continental rifting along the mid-Triassic margins of the Adria Plate, i.e., Greater Adria.
- The investigated basic calc-alkaline/shoshonitic volcanism of the NCTRB is petrogenetically and geodynamically correlated with similar rock suites found in other parts of the Dinarides, then in the Hellenides, and Albanides, as well as those from the Southern Alps and the Trans-Danubian region.

Acknowledgements: This work was supported by the Croatian Science Foundation under the project „Revealing the Middle Triassic Paleotethyan Geodynamics Recorded in the Volcano-Sedimentary Successions of NW Croatia“ (IP-2019-04-3824) and by the National Recovery and Resilience Plan 2021–2026 of the European Union – NextGenerationEU

under the project "Geodynamic evolution of the Dinaridic rift basins in the Middle Triassic". This work was partially supported by the Slovenian Research and Innovation Agency (program number P1-0011). Facilities and technical staff of the Geological Survey of Slovenia are acknowledged. The authors extend their gratitude to Josip Halamić for his valuable assistance during fieldwork. The hospitality and support of the EMPA laboratory at the University of Geneva during data acquisition are gratefully acknowledged. Critical comments and constructive reviews by Emilio Saccani and Dragan Milovanović as well as an associate editor who contributed significantly to the manuscript quality.

References

Aljinović D., Kolar-Jurkovšek T., Jurkovšek B. & Hrvatović H. 2010: Characteristics of some Middle Triassic volcaniclastic rocks in the External Dinarides (Croatia and Bosnia and Herzegovina). In: Horvat M. (Ed.): *Abstract Book. 4st Croatian Geological Congress, Šibenik*. Croatian Geological Survey, Zagreb, 14–15.

Alt J.C. & Teagle D.A.H. 2000: Hydrothermal alteration and fluid fluxes in ophiolites and oceanic crust. In: Dilek Y., Moores E.M., Elthon D. & Nicolas A. (Eds.): *Ophiolites and the Oceanic Crust: New Insights from Field Studies and the Ocean Drilling Program*. Geological Society of America, 273–282.

Aničić B. & Juriša M. 1984: *Osnovna geološka karta SFRJ 1:100 000, list Rogatec L 33-68* [Basic geological map SFRJ 1:100,000, Rogatec sheet]. Institut za geološka istraživanja, Zagreb, Savezni geološki zavod, Beograd (in Slovenian).

Aničić B. & Juriša M. 1985: *Osnovna geološka karta SFRJ 1:100 000, Tolmač za list Rogatec L 33-68* [Basic Geological Map of SFRY 1:100,000 Explanatory notes for Rogatec sheet]. Geološki zavod, Ljubljana i Institut za geološka istraživanja, Zagreb, Savezni geološki zavod, Beograd (in Slovenian).

Arculus R.J. & Powell R. 1986: Source component mixing in the regions of arc magma generation. *Journal of Geophysical Research: Solid Earth* 91, 5913–5926.

Armstrong J.T. 1991: Quantitative elemental analysis of individual microparticles with electron beam instruments. In: Heinrich K.F.J. & Newbury D.E. (Eds.): *Electron Probe Quantitation*. Springer, Boston, MA, 261–315. https://doi.org/10.1007/978-1-4899-2617-3_15

Bach W., Peucker-Ehrenbrink B., Hart S.R. & Blusztajn J. 2003: Geochemistry of hydrotermally altered oceanic crust: DSDP/ODP hole 504B – implications for seawater-crust excange budgets and Srand Pb-isotopic evolution of themantle. *Geochemistry Geophysics Geosystems* 4, 8904. https://doi.org/10.1029/2002GC000419

Balen D., Schneider P., Opitz J. & Massonne H. 2022: Pressure–temperature–time constraints on the evolution of epidote-bearing albite granite from Mt. Medvednica (Croatia): Further evidence of the Middle Triassic opening of the Neotethys Ocean. *Geologica Carpathica*, 73, 411–433. https://doi.org/10.31577/GeolCarp.73.5.2

Bébien J., Blanchet R., Cadet J.P., Charvet J., Chorowitz J., Lapierre H. & Rampnoux J.P. 1978: Le volcanisme triasique des Dinarides en Yougoslavie: sa place dans l'évolution géotectonique périméditerrenéenne. *Tectonophysics* 47, 159–176.

Beccaluva L., Di Girolamo P., Macciotta G. & Morra V. 1983: Magma affinities and fractionation trends in ophiolites. *Ofioliti* 8, 307–324.

Beccaluva L., Coltorti M., Saccani E., Siena F. & Zeda O. 2005: Triassic magmatism and Jurassic ophiolites at the margins of the Adria Plate. In: Finetti I.R. (Ed.): "*Crop Project: Deep Seismic Exploration of the Central Mediterranean and Italy*". Elsevier, 28, 607–622.

Bianchini G., Natali C., Shibata T. & Yoshikawa M. 2018: Basic dykes crosscutting the crystalline basement of Valsugana (Italy): new evidence of Early Triassic volcanism in the Southern Alps. *Tectonics* 37, 2080–2093. https://doi.org/10.1029/2017TC004950

Bonadiman C., Coltorti M. & Siena F. 1994: Petrogenesis and T-fO_2 estimates of Mt. Monzoni complex (Central Dolomites, Southern Alps): a Triassic shoshonotic intrusion in a transcurrent geodynamic setting. *European Journal of Mineralogy* 6, 943–966.

Bortolotti V. & Principi G. 2005: Tethyan ophiolites and Pangea break-up. *Island Arc* 14, 442–470. https://doi.org/10.1111/j.1440-1738.2005.00478.x

Bortolotti V., Chiari M., Marroni M., Pandolfi L., Principi G. & Saccani E. 2013: The geodynamic evolution of the ophiolites from Albania and Greece, Dinaric-Hellenic Belt: one, two, or more oceanic basins? *International Journal of Earth Sciences* 102, 783–811. https://doi.org/10.1007/s00531-012-0835-7

Capedri S., Toscani L., Grandi R., Venturelli G., Papanikolaou D. & Skarpelis N.S. 1997: Triassic volcanic rocks of some type-localities from the Hellenides. *Chemie der Erde* 57, 257–276.

Casetta F., Coltorti M. & Marrocchino E. 2018: Petrological evolution of the middle Triassic Predazzo intrusive complex, Italian Alps. *International Geology Review* 60, 977–997. https://doi.org/10.1080/00206814.2017.1363676

Casetta F., Ickert R.B., Mark D.F., Bonadiman C., Giacomoni P.P., Ntaflos T. & Coltorti M. 2019: The alkaline lamprophyres of the Dolomitic Area (Southern Alps, Italy): markers of the Late Triassic change from orogenic-like to anorogenic magmatism. *Journal of Petrology* 60, 1263–1298. https://doi.org/10.1093/petrology/egz031

Castellarin A., Lucchini F., Rossi P.L., Simboli G., Bosellini A. & Sommavilla E. 1980: Middle Triassic magmatism in southern Alps II: a geodynamic model. *Rivista Italiana di Paleontologia e Stratigrafia* 85, 3–4.

Castellarin A., Lucchini F., Rossi P.L., Selli L. & Simboli G. 1988: The Middle Triassic magmatic-tectonic arc developed in the southern Alps. *Tectonophysics* 146, 79–89.

Castorina F., Magganas A., Masi U. & Kyriakopoulos K. 2020: Geochemical and Sr–Nd isotopic evidence for petrogenesis and geodynamic setting of Lower–Middle Triassic volcanogenic rocks from central Greece: Implications for the Neotethyan Pindos ocean. *Mineralogy and Petrology* 114, 39–56. https://doi.org/10.1007/s00710-019-00687-7

Cathelineau M. 1988: Cation site occupancy in chlorites and illites as a function of temperature. *Clay Minerals* 23, 471–485.

Chen Y.L., Krystyn L., Orchard M.J., Lai X.L. & Richoz S. 2015: A review of the evolution, biostratigraphy, provincialism and diversity of Middle and early Late Triassic conodonts. *Papers in Palaeontology* 2, 235–263. https://doi.org/10.1002/spp2.1038

Chiari M., Bortolotti V., Marcucci M., Photiades A., Principi G. & Saccani E. 2012: Radiolarian biostratigraphy and geochemistry of the Koziakas massif ophiolites (Greece). *Bulletin de la Société Géologique de France* 183, 287–306. https://doi.org/10.2113/gssgfbull.183.4.287

Chicchi L., Bindi L.,Fanelli D., Tommasini S. 2023: Frontiers of thermobarometry: GAIA, a novel Deep Learning-based tool for volcano plumbing systems. *Earth and Planetary Science Letters* 620, 118352. https://doi.org/10.1016/j.epsl.2023.118352

Coombs D.S., Nakamura Y. & Vuagnat M. 1976: Pumpellyite–actinolite facies schist of the Taveyanne formation near Loeche, Valais, Switzerland. *Journal of Petrology* 17, 440–447.

Cousens B.L., Allan J.F. & Gorton M.P. 1994: Subduction-modified pelagic sediments as the enriched component in back-arc basalts from the Japan Sea. Ocean Drilling Program Sites 797 and 794. *Contribution to Mineralogy and Petrology* 117, 421–434.

Crisci C.M., Ferrara G., Mazzuoli R. & Rossi P.M. 1984: Geochemical and geochronological data on Triassic volcanism in the Southern Alps of Lombardy (Italy): genetic implications. *Geologische Rundschau* 73, 279–292.

Csontos L. & Nagymarosy A. 1998: The Mid-Hungarian line: a zone of repeated tectonic inversions. *Tectonophysics* 297, 51–71.

Dal Piaz G.V. & Martin S. 1998: Evoluzione litosferica e magmatismo nel dominio austro-sudalpino dall'orogenesivarisica al rifting permo-mesozoico. Riunione estiva S.G.I., *Memorie della Societa Geologica Italiana* 53, 43–62.

Dana J.D., Klein C. & Hurlbut C.S. 1993: *Manual of mineralogy*. Wiley, New York, 1–681.

De Min A., Velicogna M., Ziberna L., Chiaradia M., Alberti A. & Marzoli A. 2020: Triassic magmatism in the European Southern Alps as an early phase of Pangea break-up. *Geological Magazine* 157, 1800–1822. https://doi.org/10.1017/S0016756820000084

Deer W.A., Howie R.A. & Zussman J. 1992: *An introduction to the rock-forming minerals*. 2nd Edition, Prentice Hall, Harlow, 1–696.

Deer W.A., Howie R.A. & Zussman J. 2013: *An introduction to the rock-forming minerals*. 3nd Edition, Mineralogical Society of Great Britain and Ireland, London, 1–498.

Epstein A.G., Epstein J.B. & Harris L.D. 1977: Conodont Color Alteration – an Index to organic Metamorphism. *Geological Survey Professional Paper* 995, Washington, 1–27.

Faryad S.W. & Bernhardt H. 1996: Taramite-bearing metabasites from Rakovec (Gemeric Unit, The Western Carpathians). *Geologica Carpathica* 47, 349–357.

Flügel E. 2010: *Microfacies of carbonate rocks: analysis, interpretation and application*. 2nd ed., Springer, Heidelberg Dordrecht London New York, 1-984.

Gawlick H.-J., Krystyn L. & Lein R. 1994: Conodont color alteration indices: Palaeotemperatures and metamorphism in the Northern Calcareous Alps – a general view. *Geologische Rundschau* 83, 660–664.

Gill J.B. 1981: *Orogenic andesites and plate tectonics*. Springer, Berlin–Heidelberg–New York, 1–390.

Golub Lj. & Brajdić V. 1968: Basalt from Žutica near Krapina (Croatian Zagorje). *Geološki vjesnik* 21, 249–254 (in Croatian with English abstract).

Golub Lj. & Brajdić V. 1970: Eruptive and pyroclastic rocks from Vudelja and from the Bistrica brook on the northern slopes of Mt. Ivanščica (Hrvatsko Zagorje – Yugoslavia). *Zbornik radova Rudarsko-geološko-naftnog fakulteta (30. god. rada, 1939-1969)*, 123–127 (in Croatian with English abstract).

Golub Lj., Brajdić V. & Šebečić B. 1969: Eruptive and pyroclastic rocks from Mt. Strahinjščica (Croatian Zagorje). *Geološki vjesnik* 23, 205–217 (in Croatian with English abstract).

Goričan Š., Halamić J., Grgasović T. & Kolar-Jurkovšek T. 2005: Stratigraphic evolution of Triassic arc-backarc system in northwestern Croatia. *Bulletin de la Société Géologique de France* 176, 3–22.

Graciansky P.C., Roberts D.G. & Tricart P. 2011: The Western Alps, from Rift to Passive Margin to Orogenic Belt: An integrated geoscience overview. In: Shroder J.F. (Ed.): *Developments in Earth surface processes*. Elsevier, Amsterdam, 1–391.

Gradstein F.M., Ogg J.G., Schmitz M.D. & Ogg G.M. 2020: *The geologic time scale 2020*. 2 volume set, Elsevier, Amsterdam, 1–1300.

Grimes C.B., Wooden J.L., Cheadle M.J. & John B.E. 2015: "Fingerprinting" tectono-magmatic provenance using trace elements in igneous zircon. *Contribution to Mineralogy and Petrology* 170, 46. https://doi.org/10.1007/s00410-015-1199-3

Haas J., Kovács S., Gawlick H.-J., Gradinaru E., Karamata S., Sudar M., Pero C., Mello J., Polak M., Ogorelec B. & Buser S. 2011: Triassic Evolution of the Tectonostratigraphic Units of the Circum-Pannonian Region. *Jahrbuch der Geologischen Bundesanstalt* 151, 199–280.

Harangi Sz., Szabó Cs., Józsa S., Szoldán Zs., Árva-Sós E., Balla M. & Kubovics I. 1996: Mesozoic igneous suites in Hungary: Implications for genesis and tectonic setting in the northwestern part of Tethys. *International Geology Review* 38, 336–360.

Harris A.G., Lane H.R. Tailleur I.L. & Ellersiek I. 1987: Conodont thermal maturation patterns in Paleozoic and Triassic rocks, northern Alaska – geology and exploration implications. In: Tailleur I.L. & Weimar P. (Eds.): *Alaskan North Slope Geology.* Vol. I, Pacific Section, Society of Economic Paleontologists and Mineralogists, Alasko Geol. Soc., 181–191.

Hawkesworth C.J., Herft J.M., Mcdermott F. & Ellam R.M. 1991: Destructive margin magmatism and the contributions from the mantle wedge and subducted crust. *Austrian Journal of Earth Sciences* 38, 577–594.

Hawkesworth C.J., Gallagher K., Hergt J.M. & Mcdermott F. 1993: Trace element fractionation processes in the generation of island arc basalts. In: Cox K.G., Mckenzie D.P. & White R.S. (Eds.): *Melting and melt movement in the Earth*. Philosophical Transactions of Royal Society London, Oxford University Press, A342, 179–191.

Hawthorne F.C., Oberti R., Harlow G.E., Maresch W.V., Martin R.F., Schumacher J.C. & Welch M.D. 2012: Nomenclature of the amphibole supergroup. *American Mineralogist* 9, 2031–2048. https://doi.org/10.2138/am.2012.4276

Hildreth W. & Moorbath S. 1988: Crustal contributions to arc magmatism in the Andes of Central Chile. *Contribution to Mineralogy and Petrology* 98, 455–489.

Hofmann A.W. 1997: Mantle geochemistry: the message from oceanic volcanism. *Nature* 385, 219–229.

Hollocher K., Robinson P., Walsh E. & Roberts D. 2012: Geochemistry of amphibolite facies volcanics and gabbros of the Støren Nappe in extensions west and southwest of Trondheim, Western Gneiss Region, Norway: a key to correlations and paleotectonic settings. *American Journal of Science* 312, 357–416. https://doi.org/10.2475/04.2012.01

Hooper P.R., Bailey D.G. & McCarley Holder G.A. 1995: Tertiary Calc-Alkaline Magmatism Associated with Lithospheric Extension in the Pacific Northwest, *Journal of Geophysical Research* 100, 10303–10319.

Inoue A., Inoué S. & Utada M. 2018: Application of chlorite thermometry to estimation of formation temperature and redox conditions. *Clay Minerals* 53, 143–158. https://doi.org/10.1180/clm.2018.10

Jochum K.P., Willbold M., Raczek I., Stoll B. & Herwig K. 2005: Chemical characterisation of the USGS reference glasses GSA-1G, GSC-1G, GSD-1G, GSE-1G, BCR-2G, BHVO-2G and BIR-1G using EPMA, ID-TIMS, ID-ICP-MS and LA-ICP-MS. *Geostandards and Geoanalytical Research* 29, 285–302. https://doi.org/10.1111/j.1751-908X.2005.tb00901.x

Jowet E.C. 1991: Fitting Iron and Magnesium into the Hydrothermal Chlorite Geothermometer. In: *Abstracts of the GAC/MAC/SEG Joint Annual Meeting (May 27-29)*, Toronto, 16, A62.

Kamenetsky V.S., Everard J.L., Crawford A.J., Varne R., Eggins S.M. & Lanyon R. 2000: Enriched end-member of primitive MORB melts: petrology and geochemistry of glasses from Macquarie Island (SW Pacific). *Journal of Petrology* 41, 411–430. https://doi.org/10.1093/petrology/41.3.411

Kinzler R.J. 1997: Melting of mantle peridotite at pressure approaching the spinel to garnet transition: application to mid-ocean ridge basalt petrogenesis. *Journal of Geophysical Research* 102, 853–874.

Koike T. 1999: Apparatus of a Triassic conodont species *Cratognathodus multihamatus* (Huckriede). *Palaeontological Research* 3, 234–248.

Kolar-Jurkovšek T. 1983: Srednjetriasni konodonti Slovenije (Middle Triassic Conodonts from Slovenia (NW Yugoslavia)). *Rudarsko-metalurški Zbornik* 30, 323–364.

Kolar-Jurkovšek T. & Jurkovšek B. 2019: *Konodonti Slovenije (Conodonts of Slovenia)*. Geološki zavod Slovenije, Ljubljana, 1–259.

Koppers A.A.P. 2002: ArArCALC – software for $^{40}Ar/^{39}Ar$ age calculations. *Computers & Geosciences* 28, 605–619. https://doi.org/10.1016/S0098-3004(01)00095-4

Kuiper K.F., Deino A., Hilgen F.J., Krijgsman W., Renne P.R. & Wijbrans J.R. 2008: Synchronizing rock clocks of earth history. *Science* 320, 500–504. https://doi.org/10.1126/science.1154339

Kukoč D., Smirčić D., Grgasović T., Horvat M., Belak M., Japundžić Da., Kolar-Jurkovšek T., Šegvić B., Badurina L., Vukovski M. & Slovenec D. 2023: Biostratigraphy and facies description of Middle Triassic rift-related volcano-sedimentary successions at the junction of the Southern Alps and the Dinarides (NW Croatia). *International Journal of Earth Sciences* 112, 1175–1201. https://doi.org/10.1007/s00531-023-02301-w

Kukoč D., Slovenec D., Šegvić B., Vukovski M., Belak M., Grgasović T., Horvat M., Smirčić D. 2024: The early history of the Neotethys archived in the ophiolitic mélange of northwestern Croatia. *Journal of the Geological Society* 181, jgs2023-143. https://doi.org/10.1144/jgs2023-143

Le Bas M.J. 1962: The role of aluminium in igneous clinopyroxene with relation to their parentage. *American Journal of Sciences* 260, 267–288.

Leake B.E. & group of authors 1997: Nomenclature of amphiboles: Report of the Subcommittee on amphiboles of the International Mineralogical Association, Commission on new minerals and mineral names. *Canadian Mineralogist* 35, 219–246.

Ludwig K.R. 2003: Isoplot 3.09. A geochronological toolkit for Microsoft Excel. *Berkley Geochronology Center, Special Publication* 4, 1–71.

Lustrino M., Abbas H., Agostini S., Gaggiati M., Carminati E. & Gianolla P. 2019: Origin of Triassic magmatism of the Southern Alps (Italy): constraints from geochemistry and Sr–Nd–Pb isotopic ratios. *Gondwana Research* 75, 218–238. https://doi.org/10.1016/j.gr.2019.04.011

Marci V., Šćavničar S. & Sijarić G. 1982: Petrogenesis of the volcanic rocks of Ivanščica Mt. (River Željeznica). X kongres geologa Jugoslavije, Budva. *Zbornik radova* 1, 329–335 (in Croatian with English summary).

Marci V., Ščavnićar S. & Sijarić G. 1984: The new data about volcanic rocks of Ivanščica mountain. *Geološki Vjesnik* 37, 97–104 (in Croatian with English abstract).

Márton E., Pavelić D., Tomljenović B., Avanić R., Pamić J. & Márton P. 2002: In the wake of a counterclockwise rotating Adriatic microplate: Neogene paleomagnetic results from Northern Croatia. *International Journal of Earth Sciences* 91, 514–523. https://doi.org/10.1007/s00531-001-0249-4

McDonough W.F. & Frey F.A. 1989: REE in upper mantle rocks. In: Lipin B. & Mckay G.R. (Eds.): *Geochemistry and mineralogy of rare earth elements*. Mineralogical Society of America, Chelsea, Michigan, 99–145.

McKenzie D.P. & O'Nions R.K. 1991: Partial melt distributions from inversion of rare earth element concentrations. *Journal of Petrology* 32, 1027–1091.

Monjoie P., Lapierre H., Tashko A., Mascle G.H., Dechamp A., Muceku B. & Brunet P. 2008: Nature and origin of the Triassic volcanism in Albania and Othrys: a key to understanding the Neotethys opening? *Bulletin de la Société Géologique de France* 179, 411–425.

Morimoto N. 1988: Nomenclature of pyroxenes. *Schweizeriche Mineralogische und Petrographische Mitteilungen* 68, 95–111.

Mrdak M., Đaković M., Gawlick H-J., Djerić N., Bucur I.I., Sudar M., Milić M. & Čađenović D. 2024: Middle Triassic stepwise deepening and stratigraphic condensation associated with Illyrian volcanism in the Durmitor Mountain, Montenegro. *Facies* 70, 10. https://doi.org/10.1007/s10347-024-00683-0

Müller D., Rock N.M.S. & Groves D.I. 1992: Geochemical discrimination between shoshonitic and potassic volcanic rocks in different tectonic settings: A pilot study. *Mineralogy and Petrology* 46, 259–289.

Nardini N., Casseta F., Ickert R.B., Tavazzani L., Okhai D.C., Peres S., Dellantonio E., Ntaflos T. & Coltorti M. 2025: The timing of the Middle Triassic magmatism in the Dolomites area (Southern Alps, Italy): U–Pb geochronology of zircon and titanite hosted in plutonic rocks and phonolite dykes. *Lithos* 494–495, 107894. https://doi.org/10.1016/j.lithos.2024.107894

Neave D.A. & Putirka K.D. 2017: A new clinopyroxene-liquid barometer, and implications for magma storage pressures under Icelandic rift zones. *American Mineralogist* 102, 777–794. https://doi.org/10.2138/am-2017-5968

Neubauer F., Liu Y., Cao S. & Yuan S. 2019: What is the Austroalpine mega-unit and what are the potential relations to Paleotethys Ocean remnants of southeastern Europe? In: *Proceedings of the Geologica Carpathica 70 Conference*. Earth Science Institute of the Slovak Academy of Sciences, Bratislava, 16–20.

Nimis P. 1999: Clinopyroxene geobarometry of magmatic rocks. Part 2: Structural geobarometers for basic to acid, tholeiitic and mildly alkaline magmatic systems. *Contribution to Mineralogy and Petrology* 135, 62–74.

Nimis P. & Ulmer P. 1998: Clinopyroxene geobarometry of magmatic rocks. Part 1: an expanded structural geobarometer for anhydrous and hydrous, basic and ultrabasic systems. *Contribution to Mineralogy and Petrology* 133, 122–135.

Obenholzner J.H. 1991: Triassic volcanogenic sediments from the Southern Alps (Italy, Austria, Yugoslavia) – a contribution to the "Pietra verde" problem. *Sedimentary Geology* 74, 147–171.

Ogg J.G., Ogg G. & Gradstein F.M. 2016: *A concise geological time scale*. Elsevier, Amsterdam, 1–240.

Ogunyele A.C., Bonazzi M., Giovanardi T., Mazzucchelli M., Salters V.J.M., Decarlis A., Sanfilippo A. & Zanetti A. 2024: Transition from orogenic-like to anorogenic magmatism in the Southern Alps during the Early Mesozoic: evidence from elemental and Nd–Sr–Hf–Pb isotope geochemistry of alkali-rich dykes from the Finero phlogopite peridotite, Ivrea–Verbano Zone. *Gondwana Research* 129, 201–219. https://doi.org/10.1016/j.gr.2023.12.011

Pamić J. 1984: Triassic magmatism of the Dinarides in Yugoslavia. *Tectonophysics* 109, 273–307.

Pamić J. & Balen D. 2005: Interaction between Permo-Triassic rifting, magmatism and initiation of the Adriatic-Dinaridic carbonate platform (ADCP). *Acta Geologica Hungarica* 48, 181–204.

Pamić J. & Tomljenović B. 1998: Basic geological data on the Croatian part of the Mid-Transdanubian Zone as exemplified by Mt. Medvednica located along the Zagreb-Zemplen Fault Zone. *Acta Geologica Hungarica* 41, 389–400.

Pe-Piper G. 1998: The nature of Triassic extension-related magmatism in Greece: Evidence from Nd and Pb isotope geochemistry. *Geological Magazine* 135, 331–348.

Pe-Piper G. & Mavronichi M. 1990: Petrology, geochemistry and regional significance of the Triassic volcanic rocks of the Western Parnassos isotopic zone of Greece. *Ofioliti* 15, 269–285.

Pe-Piper G. & Panagos A.G. 1989: Geochemical characteristics of the Triassic Volcanic rocks of Evia: Petrogenetic and tectonic Implications. *Ofioliti* 14, 33–50.

Pearce J.A. 1975: Basalt geochemistry used to investigate past tectonic environments on Cyprus. *Tectonophysics* 25, 41–67.

Pearce J.A. 1982: Trace element characteristics of lavas from destructive plate boundaries. In: Thorpe R.S. (Ed.): *Andesites*. Wiley, New York, 525–548.

Pearce J.A. 1983: Role of the sub-continental lithosphere in magma genesis at active continental margins. In: Hawkesworth C.J. & Norry M.J. (Eds.): Continental basalts and mantle xenoliths. *Shiva*, Nantwich UK, 230–249.

Pearce J.A. 1996: A user's guide to basalt discrimination diagrams. In Trace Element Geochemistry of Volcanic Rocks: Applications for Massive Sulphide Exploration. In: Wyman D.A. (Ed.): *Short Course Notes* 12. Geological Association of Canada, Newfoundland, NL, Canada, 79–113.

Pearce J.A. & Norry M.J. 1979: Petrogenetic Implications of Ti, Zr, Y, and Nb variations in volcanic rocks. *Contributions to Mineralogy and Petrology* 69, 33–47.

Pearce J.A., Lippard S.J. & Roberts S. 1984: Characteristics and tectonic significance of supra-subduction zone ophiolites. In: Kokelaar B.P. & Howells M.F. (Eds.): Marginal Basin Geology: Volcanic and Associated Sedimentary and Tectonic Processes in Modern and Ancient Marginal Basins. *Geological Society, London, Special Publication* 16, 17–94.

Pearce J.A., Baker P.E., Harvey P.K. & Luff I.W. 1995: Geochemical evidence for subduction flukses, mantle melting for fractional crystalization beneath the South Sandwich Island Arc. *Journal of Petrology* 36, 1073–1109.

Peate D.W., Pearce J.A., Hawkesworth C.J., Colley H., Edwards M.H. & Hirose K. 1997: Geochemical variations in Vanuatu Arc lavas: the role of subducted material and a variable mantle wedge composition. *Journal of Petrology* 38, 1331–1358.

Placer L. 1999: Structural meaning of the Sava folds. *Geologija* 41, 191–221.

Plank T. 2005: Constraints from thorium/lanthanumon sediment recycling at subduction zones and the evolution of the continents. *Journal of Petrology* 46, 921–944. https://doi.org/10.1093/petrology/egi005

Plank T. & Langmuir C.H. 1998: The chemical composition of subducting sediment and its consequences for the crust and mantle. *Chemical Geology* 145, 325–394. https://doi.org/10.1016/S0009-2541(97)00150-2

Pomonis P., Tsikouras V. & Hatzipanagiotou K. 2004: Comparative geochemical study of the Triassic trachyandesites of Glykomilia and alkali basalts from the Koziakas ophiolite mélange (W. Thessaly): implications for their origin. *Bulletin of the Geological Society of Greece* 36, 587–596.

Radulović N., Milovanović D., Čađenović D. & Đaković M. 2014: Occurrence of peperite in the southeastern part of Montenegro. *Proceedings of the XVI Serbian Geological Congress*, Donji Milanovac, 22–25 May 2014, 295–296.

Rahn M., Mullis J., Erdelbrock K. & Frey M. 1994: Very low-grade metamorphism of the Taveyanne greywacke, Glarus Alps, Switzerland. *Journal of Metamorphic Geology* 12, 625–641.

Rejebia V.A., Harris A.G. & Huebner J.S. 1987: Conodont color and textural alteration: An index to regional metamorphism, contact metamorphism, and hydrothermal alteration. *Bulletin of the Geological Society of America* 99, 471–479.

Rigo M., Mazza M., Karádi V. & Nicora A. 2018: New Upper Triassic Conodont Biozonation of the Tethyan Realm. Chapter 6. In: Tanner L.H. (Ed.): The Late Triassic World. *Topics in Geobiology* 46, 189–235. https://doi.org/10.1007/978-3-319-68009-5_6

Saccani E. 2015: A new method of discriminating different types of post-Archean ophiolitic basalts and their tectonic significance using Th–Nb and Ce–Dy–Yb systematics. *Geoscience Frontiers* 6, 481–501. https://doi.org/10.1016/j.gsf.2014.03.006

Saccani E., Dilek Y., Marroni M. & Pandolfi L. 2015: Continental margin ophiolites of Neotethys: Remnants of Ancient Ocean–Continent Transition Zone (OCTZ) lithosphere and their geochemistry, mantle sources and melt evolution patterns. *Episodes* 38, 230–249. https://doi.org/10.18814/epiiugs/2015/v38i4/82418

Schmidt M.W. & Jagoutz O. 2017: The global systematics of primitive arc melts. *Geochemistry, Geophysics, Geosystems*, 18, 2817–2854. https://doi.org/10.1002/2016GC006699

Schmid S.M., Fügenschuh B., Kissling E. & Schuster R. 2004: Tectonic map and overall architecture of the Alpine orogen. *Eclogae Geologicae Helvetiae* 97, 93–117. https://doi.org/10.1007/s00015-004-1113-x

Schmid S.M., Bernoulli D., Fügenschuh B., Matenco L., Scheffer S., Schuster R., Tischler M. & Ustaszewski K. 2008: The Alpine–Carpathian-Dinaridic orogenic system: correlation and evolution of tectonic units. *Swiss Journal of Geosciences* 101, 139–183. https://doi.org/10.1007/s00015-008-1247-3

Schmid S.M., Fügensschuh B., Kounov A. et al. 2020: Tectonic units of the Alpine collision zone between Eastern Alps and western Turkey. *Gondwana Research* 78, 308–374. https://doi.org/10.1016/j.gr.2019.07.005

Šebečić B. 1969: Sedimentary rocks of Strahinjščica Mountain. *Geološki Vjesnik* 23, 241–256 (in Croatian with English abstract).

Šegvić B., Slovenec Da. & Badurina L. 2023a: Major and rare earth element mineral chemistry of low-grade assemblages inform dynamics of hydrothermal ocean-floor metamorphism in the Dinaridic Neotethys. *Geological Magazine* 160, 444–470. https://doi.org/10.1017/S0016756822001030

Šegvić B., Lukács R., Mandic O., Strauss P., Badurina L., Guillong M. & Harzhauser M. 2023b: U–Pb zircon age and mineralogy of St. Georgen halloysite tuff shed light on the timing of the middle Badenian (mid-Langhian) transgression, ash dispersal, and paleoenvironmental conditions in the southern Vienna Basin, Austria. *Journal of the Geological Society* 180, jgs2022-106. https://doi.org/10.1144/jgs2022-106

Şengör A.M.C. 1984: The Cimmeride orogenic system and the tectonics of Eurasia. *Geological Society of America Special Paper* 195, 1–82.

Şengör A.M.C. 2009: Tectonic evolution of the Mediterranean: a dame with four husbands. *Trabajos de Geología* 29, 45–50.

Serri G., Innocenti F. & Manetti P. 2001: Magmatism from Mesozoic to Present: petrogenesis, time-space distribution and geodynamic implications. In: Vai G.B. & Martini I.P. (Eds.): *Anatomy of an Orogen: The Apennines and Adjacent Mediterranean Basins*. Kluwer Academic Publishers, 77–104.

Šimunić An. & Šimunić Al. 1997: Triassic Deposits of Hrvatsko Zagorje. *Geologia Croatica* 50, 243–250.

Šimunić An., Pikija M., Hećimović I. & Šimunić Al. 1981: *Osnovna geološka karta SFRJ 1:100 000, Tumač za list Varaždin L 33-69* [Basic Geological Map of SFRY 1:100,000 Explanatory notes for Varaždin sheet]. Institut za geološka istraživanja, Zagreb, Savezni geološki zavod, Beograd.

Šimunić An., Pikija M. & Hećimović I. 1982: *Osnovna geološka karta SFRJ 1:100 000, list Varaždin* [Basic Geological Map of SFRY 1:100,000, Varaždin sheet]. Institut za geološka istraživanja, Zagreb, Savezni geološki zavod, Beograd (in Croatian).

Slovenec Da. & Šegvić B. 2021: Middle Triassic high-K calc-alkaline effusive and pyroclastic rocks from the Zagorje-Mid-Transdanubian Zone (Mt. Kuna Gora; NW Croatia): Mineralogy, petrology, geochemistry and tectono-magmatic affinity. *Geologica Acta* 19, 1–23. https://doi.org/10.1344/GeologicaActa2021.19.2

Slovenec Da. & Šegvić B. 2024: The evolution of the Mesozoic lithosphere of northwestern Neotethys: A petrogenetic and geodynamic perspective. *Journal of the Geological Society* 181, jgs2023-132. https://doi.org/10.1144/jgs2023-132

Slovenec Da., Lugović B. & Vlahović I. 2010: Geochemistry, petrology and tectonomagmatic significance of basaltic rocks from the ophiolite mélange at the NW External-Internal Dinarides junction (Croatia). *Geologica Carpathica* 61, 273–294. https://doi.org/10.2478/v10096-010-0016-1

Slovenec Da., Lugović B., Meyer P. & Garapić-Šiftar G. 2011: A tectono-magmatic correlation of basaltic rocks from ophiolite mélanges at the north-eastern tip of the Sava-Vardar suture Zone, Northern Croatia, constrained by geochemistry and petrology. *Ofioliti* 36, 77–100. https://doi.org/10.4454/ofioliti.v36i1.395

Slovenec Da., Šegvić B., Halamić J., Goričan Š. & Zanoni G. 2020: An ensialic volcanic arc along the northwestern edge of Palaeotethys-Insights from the Mid-Triassic volcanosedimentary succession of Ivanščica Mt. (northwestern Croatia). *Geological Journal* 55, 4324–4351. https://doi.org/10.1002/gj.3664

Slovenec Da., Horvat M., Smirčić D., Belak M., Badurina L., Kukoč D., Grgasović T., Byerly K., Vukovski M. & Šegvić B. 2023a: On the evolution of Middle Triassic passive margins of the Greater Adria Plate: inferences from the study of calc-alkaline and shoshonitic tuffs from NW Croatia. *Ofioliti* 58, 31–46. https://doi.org/10.4454/ofioliti.v48i1.560

Slovenec Da., Belak M., Badurina L., Horvat M. & Šegvić B. 2023b: Triassic evolution of the Adriatic-Dinaridic platform's continental margins – insight from rare dolerite subvolcanic intrusions in External Dinarides, Croatia. *Comptes Rendus Geoscience* 355, 35–62. https://doi.org/10.5802/crgeos.183

Smirčić D., Kolar-Jurkovšek T., Aljinović D., Barudžija U., Jurkovšek B. & Hrvatović H. 2018: Stratigraphic definition and correlation of the Middle Triassic volcaniclastic facies in the External Dinarides: Croatia and Bosnia and Herzegovina. *Journal of Earth Sciences* 29, 864–878. https://doi.org/10.1007/s12583-018-0789-1

Smirčić D., Aljinović D., Barudžija U. & Kolar-Jurkovšek T. 2020: Middle Triassic syntectonic sedimentation and volcanic influence in the central part of the External Dinarides, Croatia (Velebit Mts.). *Geological Quarterly* 64, 220–239.

Smirčić D., Vukovski M., Slovenec Da., Kukoč D., Šegvić B., Horvat M., Belak M., Grgasović T. & Badurina L. 2024: Facies architecture, geochemistry and petrogenesis of Middle Triassic volcaniclastic deposits of Mt. Ivanščica (NW Croatia): evidence of bimodal volcanism in the Alpine-Dinaridic transitional zone. *Swiss Journal of Geosciences* 117, art. no 5. https://doi.org/10.1186/s00015-024-00453-8

Spahić D. 2024: Elusive Permian – Triassic Western Paleotethyan paleogeography: Towards the Early Cimmerian pre-Vardar configuration (Dinarides-Carpathian Balkan Belt). *Earth Science Review* 256, 104857. https://doi.org/10.1016/j.earscirev.2024.104857

Stampfli G.M. & Borel G.D. 2002: A plate tectonic model for the Paleozoic and Mesozoic constrained by dinamic plate boundaries and restored synthetic ocean isochrons. *Earth and Planetary Science Letters* 196, 17–33. https://doi.org/10.1016/S0012-821X(01)00588-X

Stampfli G.M. & Borel G.D. 2004: The TRANSMED transects in space and time: Constraints on the paleotectonic evolution of the Mediterranean domain. In: Cavazza W., Roure F., Spakman W., Stampfli G.M. & Ziegler P.A. (Eds.): *The TRANSMED Atlas: the Mediterranean Region from crust to mantle*. Springer-Verlag, Berlin, 53–80.

Stampfli G.M. & Hochard C. 2009: Plate tectonics of the Alpine realm. *Geological Society, London, Special Publications* 327, 89–111. https://doi.org/10.1144/SP327.6

Stampfli C., Hochard C., Vérard C., Wilhem J. & von Raumer J.F. 2013: The formation of Pangea. *Tectonophysics* 593, 1–19. https://doi.org/10.1016/j.tecto.2013.02.037

Storck J.C., Brack P., Wotzlaw J.F. & Ulmer P. 2018: Timing and evolution of Middle Triassic magmatism in the Southern Alps (Northern Italy). *Journal of the Geological Society* 176, 253–268. https://doi.org/10.1144/jgs2018-123

Sudar M. 1986: Triassic microfossils and biostratigraphy of the Inner Dinarides between Gučevo and Ljubišnja Mts., Yugoslavia, *Geološki anali Balkanskog poluostrva* 50, 151–394.

Sudar M.N. & Budurov K. 1979: New conodonts from the Triassic in Yugoslavia and Bulgaria. *Geologica Balcanica* 9, 47–52.

Sudar M.N., Gawlick H.J., Lein R., Missoni S., Kovács S. & Jovanović D. 2013: Depositional environment, age and facies of the Middle Triassic Bulog and Rid formations in the Inner Dinarides (Zlatibor Mountain, SW Serbia): evidence for the Anisian break-up of the Neotethys Ocean. *Neues Jahrbuch für Geologie und Paläontologie Abhandlungen* 269, 291–320. https://doi.org/10.1127/0077-7749/2013/0352

Sudar M., Gawlick H-J., Bucur I.I., Jovanović D., Missoni S.† & Lein L. 2023: From shallow-water carbonate ramp to hemipelagic deep-marine carbonate deposition: part 3. Lithostratigraphy and formations of the Middle to Late Anisian Bulog sedimentary successions (Bulog Group) in the Dinarides (Bosnia and Herzegovina, Serbia, Montenegro). *Geološki anali Balkanskoga poluostrva* 84, 71–106.

Sun S.S. & McDonough W.F. 1989: Chemical and isotopic systematics of oceanic basalts: implications for mantle composition and processes. In: Saunders A.D. & Norry M.J. (Eds.): Magmatism in Ocean Basins. *Geological Society, London, Special Publication* 42, 313–345.

Swinden H.S., Jenner G.A., Fryer B.J., Hertogen J. & Roddick J.C. 1990: Petrogenesis and paleotectonic history of the Wild Bight Group, an Ordovician rifted island arc in central Newfoundland. *Contribution to Mineralogy and Petrology* 105, 219–241.

Tanaka T., Togashi S., Kamioka H., Amakawa H., Kagami H., Hamamoto T., et al. 2000: JNdi-1: A neodymium isotopic reference in consistency with Lajolla neodymium. *Chemical Geology* 168, 279–281. https://doi.org/10.1016/S0009-2541(00)00198-4

Taylor S.R. & McLennan S.M. 1985: The continental crust: its composition and evolution. *Blackwell Scientific Publication*, Oxford, 1–312.

Tillick D.A., Peacor D.R. & Mauk J.L. 2001: Genesis of dioctahedral phyllosilicates during hydrothermal alteration of volcanic rocks: I. The Golden Cross epithermal ore deposit, New Zealand. *Clay and Clay Minerals* 49, 126–140.

Tomljenović B., Csontos L., Márton E. & Márton P. 2008: Tectonic evolution of the northwestern Internal Dinarides as constrained by structures and rotation of Medvednica Mountains, North Croatia. *Geological Society, London, Special Publications* 298, 145–167. https://doi.org/10.1144/SP298.8

Trubelja F., Burgath K.P. & Marchig V. 2004: Triassic magmatism in the area of the Central Dinarides (Bosnia and Herzegovina): Geochemical Resolving of tectonic setting. *Geologia Croatica* 57, 159–170.

Ustaszewski K., Schmid S.M., Lugović B., Schuster R., Schaltegger U., Bernoulli D., Hottinger L., Kounov A., Fügenschuh B. & Schefer S. 2009: Late Cretaceous intra-oceanic magmatism in the internal Dinarides (northern Bosnia and Herzegovina): Implications for the collision of the Adriatic and European plates. *Lithos* 108, 106–125. https://doi.org/10.1016/j.lithos.2008.09.010

van Hinsbergen J.J. & Schouten T.L.A. 2021: Deciphering paleogeography from orogenic architecture: constructing orogens in a future supercontinent as thought experiment. *American Journal of Science* 321, 955–1031. https://doi.org/10.2475/06.2021.09

van Hinsbergen D.J.J., Torsvik T.H., Schmid S.M., Maţenco L.C., Maffione M., Vissers R.L.M., Gürer D. & Spakman W. 2020: Orogenic architecture of the Mediterranean region and kinematic reconstruction of its tectonic evolution since the Triassic. *Gondwana Research* 81, 79–229. https://doi.org/10.1016/j.gr.2019.07.009

Velicogna M., De Min A., Prašek M.K., Ziberna L., Brombin V., Jourdan F., Renne P.R., Balen D., Grégoire, M. & Marzoli A. 2023: The Norian magmatic rocks of Jabuka, Brusnik and Vis

Islands (Croatia) and their bearing on the evolution of Triassic magmatism in the Northern Mediterranean. *International Geology Review* 65, 2558–2579. https://doi.org/10.1080/00206814.2022.2150898

Velledits F. 2006: Evolution of Bükk Mountains (NE Hungary) during the Middle-Late Triassic asymmetric rifting of the Vadar-Meliata branch of the Neotethys Ocean. *International Journal of Earth Sciences* 95, 395–412. https://doi.org/10.1007/s00531-005-0041-y

Vidal O., Lanari P., Munoz M., Bourdelle F. & Andrade V.D. 2016: Deciphering temperature, pressure and oxygen-activity conditions of chlorite formation. *Clay Minerals* 51, 615–633.

Vidal O., Parra T. & Vieillard P. 2005: Thermodynamic properties of the Tschermak solid solution in Fe-chlorite: Application to natural examples and possible role of oxidation. *American Mineralogist* 90, 347–358.

Visona D., Nimis P., Cavazzini G., Fioretti A.M., Laurenzi M.A., Massironi M. & Villa I.M. 2025: Alkaline magmatism in the post-orogenic Triassic Predazzo complex, Dolomites, NE Italy: Ages and significance. *Lithos* 494–495, 107912. https://doi.org/10.1016/j.lithos.2024.107912

Vukovski M., Kukoč D., Grgasović T., Fuček L. & Slovenec Da. 2023: Evolution of eastern passive margin of Adria recorded in shallow- to deep-water successions of the transition zone between the Alps and the Dinarides (Ivanščica Mt., NW Croatia). *Facies* 69, 18.

Vukovski M., Špelić M., Kukoč D., Troskot-Čorbić T., Grgasović T., Slovenec Da. & Tomljenović B. 2024: Unravelling the tectonic evolution of the Dinarides-Alps-Pannonian Basin transition zone: insights from structural analysis and low-temperature thermochronology from Ivanščica Mt., NW Croatia. *Swiss Journal of Geosciences* 117, 16. https://doi.org/10.1186/s00015-024-00464-5

Vukovski M., Slovenec Da., Belak M., Šegvić B., Mišur I., Smirčić D., Horvat M., Kukoč D., Grgasović T. & Slivšek G. 2026: Middle Triassic ignimbrites as markers of Eoalpine high-pressure metamorphism and large-scale lateral extrusion of Adria derived units at the edge of the European Alps. *Solid Earth* [accepted], https://doi.org/10.5194/egusphere-2026-1092

Walter M.J. 1998: Melting of garnet peridotite and the origin of komatiite and depleted lithosphere. *Journal of Petrology* 39, 29–60.

Wang X.-C., Xu B.,Wilde S.A. & Pang C.J. 2016: Origin of arc-like continental basalts: Implications for deep-Earth fluid cycling and tectonic discrimination. *Lithos* 261, 5–45. https://doi.org/10.1016/j.lithos.2015.12.014

Wang Z., Chen B., Yan X. & Li S. 2018: Characteristics of hydrothermal chlorite from the Niujuan Ag-Au-Pb-Zn deposit in the north margin of NCC and implications for exploration tools for ore deposits. *Ore Geology Reviews* 101, 398–412. https://doi.org/10.1016/j.oregeorev.2018.08.003

Weis D., Kieffer B., Maerschalk C., Barling J., de Jong J., Willians G.A., Hanano D., Pretorius W., Scoates J.S., Goolaerts A., Friedman R.M. & Mahoney J.B. 2006: High-precision isotopic characterization of USGS reference materials by TIMS and MC-ICP-MS. *Geochemistry, Geophysics, Geosystems* 7, 1–30. https://doi.org/10.1029/2006GC001283

Whitney D.L. & Evans B.W. 2010: Abbreviations for names of rock-forming minerals. *American Mineralogist* 95, 185–187. https://doi.org/10.2138/am.2010.3371

Wilson M. 1989*: Igneous petrogenesis*. Unwin Hyman Ltd., London, 1–466.

Winkler H.G.H. 1979: *Petrogenesis of metamorphic rocks*. 5th edition, Springer Verlag, Berlin, 1–348.

Wood D.A. 1980: The application of a Th-Hf-Ta diagram to problems of tectonomagmatic classification and establishing the nature of crustal contamination of basaltic lavas of the British Tertiary volcanic province. *Earth and Planetary Science Letters* 50, 11–30.

Workman R.K. & Hart S.R. 2005: Major and trace element composition of the depleted MORB mantle (DMM). *Earth and Planetary Science Letters* 231, 53–72. https://doi.org/10.1016/j.epsl.2004.12.005

Zane A. & Weiss Z.A. 1998: Procedure for classifying rock-forming chlorites based on microprobe data. *Rendiconti Lincei* 9, 51–56.

Zindler A. & Hart S.R. 1986: Chemical geodynamics. *Annual Review of Earth and Planetary Sciences* 14, 439–571.

Zulauf G., Dörr W., Marko L. & Krahl J. 2018: The late Eo-Cimmerian evolution of the external Hellenides: constraints from microfabrics and U–Pb detrital zircon ages of Upper Triassic (meta) sediments (Crete, Greece). *International Journal of Earth Sciences* 107, 2859–2894. https://doi.org/10.1007/s00531-018-1632-8

Electronic supplementary material is available online:
Supplementary Fig. S1 at https://geologicacarpathica.com/data/files/supplements/GC-77-4-Slovenec_FigS1.tif
Supplementary Fig. S2 at https://geologicacarpathica.com/data/files/supplements/GC-77-4-Slovenec_FigS2.tif
Supplementary Table S1 at https://geologicacarpathica.com/data/files/supplements/GC-77-4-Slovenec_TableS1.docx
Supplementary Table S2 at https://geologicacarpathica.com/data/files/supplements/GC-77-4-Slovenec_TableS2.docx
Supplementary Table S3 at https://geologicacarpathica.com/data/files/supplements/GC-77-4-Slovenec_TableS3.docx
Supplementary Table S4 at https://geologicacarpathica.com/data/files/supplements/GC-77-4-Slovenec_TableS4.docx
Supplementary Table S5 at https://geologicacarpathica.com/data/files/supplements/GC-77-4-Slovenec_TableS5.docx